AD-A173 210 HIGH TEMPERATURE OXIDATION STUDIES ON ALLOYS CONTAINING 1/1
DISPERSED PHASE P..(U) PENNSYLVANIA STATE UNIV
UNIVERSITY PARK DEPT OF MATERIALS SCI.. G SIMKOVICH
UNCLASSIFIED 28 AUG 86 AFOSR-TR-86-0836 F/G 11/6 NL

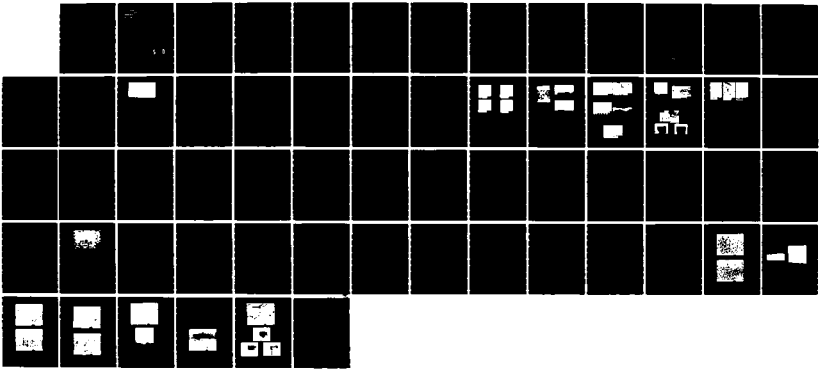

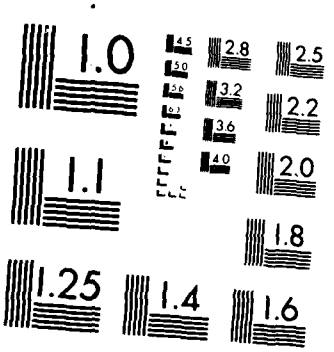

(2)

COLLEGE OF EARTH AND MINERAL SCIENCES

Grant No. AFOSR-85-0298

First Annual Report

Approved for public release; distribution unlimited.

to

Air Force Office of Scientific Research
Bolling, AFB, DC 20332

HIGH TEMPERATURE OXIDATION STUDIES ON ALLOYS CONTAINING DISPERSED PHASE PARTICLES AND CLARIFICATION OF THE MECHANISM OF GROWTH OF SiO_2

Submitted to: Maj. Joseph W. Hager

Submitted by: G. Simkovich

August 1986

The Pennsylvania State University
University Park, Pennsylvania

THE PENNSYLVANIA STATE UNIVERSITY

College of Earth and Mineral Sciences

UNDERGRADUATE PROGRAMS OF STUDY

Ceramic Science and Engineering, Earth Sciences, Fuel Science, Geography, Geosciences, Metallurgy, Meteorology, Mineral Economics, Mining Engineering, Petroleum and Natural Gas Engineering, and Polymer Science.

GRADUATE PROGRAMS AND FIELDS OF RESEARCH

Ceramic Science, Fuel Science, Geochemistry and Mineralogy, Geography, Geology, Geophysics, Metallurgy, Meteorology, Mineral Economics, Mineral Processing, Mining Engineering, Petroleum and Natural Gas Engineering, and Polymer Science.

UNIVERSITY-WIDE INTERDISCIPLINARY GRADUATE PROGRAMS INVOLVING E&MS FACULTY AND STUDENTS

Earth Sciences, Ecology, Environmental Pollution Control Engineering, Mineral Engineering Management, Operations Research, Regional Planning, and Solid State Science.

ASSOCIATE DEGREE PROGRAMS

Metallurgical Engineering Technology and Mining Technology.

INTERDISCIPLINARY RESEARCH GROUPS WITHIN THE COLLEGE

Coal Research, Ore Deposits Research, Earth System Science, and the Mining and Mineral Resources Research Institute.

ANALYTICAL AND STRUCTURAL STUDIES

Classical chemical analysis of metals and silicate and carbonate rocks; X-ray crystallography; electron microscopy and diffraction; electron microprobe analysis; atomic absorption analysis; spectrochemical analysis; surface analysis by secondary ion mass spectrometry (SIMS); and scanning electron microscopy (SEM).

U.Ed. 9-725

SECURITY CLASSIFICATION OF THIS PAGE

REPORT DOCUMENTATION PAGE

1a. REPORT SECURITY CLASSIFICATION	1b. RESTRICTIVE MARKINGS
2a. SECURITY CLASSIFICATION AUTHORITY	3. DISTRIBUTION/AVAILABILITY OF REPORT
2b. DECLASSIFICATION/DOWNGRADING SCHEDULE	
4. PERFORMING ORGANIZATION REPORT NUMBER(S)	5. MONITORING ORGANIZATION REPORT NUMBER(S)
6a. NAME OF PERFORMING ORGANIZATION: Dept. of Mat. Sci. & Eng. The Pennsylvania State Univ. / 6b. OFFICE SYMBOL (If applicable)	7a. NAME OF MONITORING ORGANIZATION: AFOSR
6c. ADDRESS (City, State and ZIP Code): 206-B Steidle Building University Park, PA 16802	7b. ADDRESS (City, State and ZIP Code): Bld 410 BAFB DC 20332
8a. NAME OF FUNDING/SPONSORING ORGANIZATION: AFOSR / 8b. OFFICE SYMBOL (If applicable): NE	9. PROCUREMENT INSTRUMENT IDENTIFICATION NUMBER: AFOSR-85-0298
8c. ADDRESS (City, State and ZIP Code): Bolling AFB Washington, D.C. 20332	10. SOURCE OF FUNDING NOS.

PROGRAM ELEMENT NO.	PROJECT NO.	TASK NO.	WORK UNIT NO.
~~AFOSR~~ 61102F	~~85-0298~~ 2306	A2	

11. TITLE (Include Security Classification): High Temperature Oxidation . . . . . of Growth of SiO_2	
12. PERSONAL AUTHOR(S): G. Simkovich	

13a. TYPE OF REPORT	13b. TIME COVERED	14. DATE OF REPORT (Yr., Mo., Day)	15. PAGE COUNT
1st Annual	FROM 15Aug85 TO 14Aug86	1986 Aug 28	

16. SUPPLEMENTARY NOTATION

17. COSATI CODES			18. SUBJECT TERMS (Continue on reverse if necessary and identify by block number)
FIELD	GROUP	SUB. GR.	

19. ABSTRACT (Continue on reverse if necessary and identify by block number)

A wide variety of high temperature oxidation tests have been conducted on Fe, Co and Ni based alloys. Results are discussed and several papers submitted for publication are appended.

20. DISTRIBUTION/AVAILABILITY OF ABSTRACT: UNCLASSIFIED/UNLIMITED ☐ SAME AS RPT ☐ DTIC USERS ☐	21. ABSTRACT SECURITY CLASSIFICATION

22a. NAME OF RESPONSIBLE INDIVIDUAL	22b. TELEPHONE NUMBER (Include Area Code)	22c. OFFICE SYMBOL
		NE

DD FORM 1473, 83 APR EDITION OF 1 JAN 73 IS OBSOLETE.

SECURITY CLASSIFICATION OF THIS PAGE

Grant No. AFOSR-85-0298

First Annual Report

to

Air Force Office of Scientific Research
Bolling, AFB, DC 20332

HIGH TEMPERATURE OXIDATION STUDIES ON ALLOYS CONTAINING DISPERSED PHASE PARTICLES AND CLARIFICATION OF THE MECHANISM OF GROWTH OF SiO_2

Submitted to: Maj. Joseph W. Hager

Submitted by: G. Simkovich

August 1986

Introduction

This report summarizes the work performed at The Pennsylvania State University during the period 15 Aug 1985 to 14 Aug 1986 under Grant No. AFOSR-85-0298. The project was directed by Prof. George Simkovich. Others that have contributed to the program are the following graduate students: C. Buss, D. H. Kim, B. Munn, S. W. Park, M. Y. Su and G. P. Wagner. Mr. Munn and Mr. Park have worked directly as 1/2 time research assistants on this grant while the other students have aided via interaction with Kim, Munn and Park or by aiding in the experimental program.

In this report we summarize the initial efforts on the project which includes the experimental arrangements and results obtained. Several papers that have been submitted for publication are included in this report as appendices.

Annual Report - 1st year - 15 Aug 85 - 14 Aug 86

Summary of Results

Experimental Arrangement

In order to properly monitor the high temperature oxidation kinetics a thermal gravimetric analysis (TGA) system was constructed. This included a gas flowmeter system, furnace and a balance coupled to a computer to collect and partially analyze the data. Additional facilities utilized, e.g. optical microscopes, SEM, etc, were primarily in place.

The gas flowmeter system is capable of supplying to the reaction chamber a variety of gas mixtures. However, the oxidation experiments described in this report were all conducted at 1 atmosphere of oxygen since this represents a standard against which most materials are frequently measured.

The furnace assembly was constructed internally. It consists of a temperature controller and a furnace tube heated by SiC heating elements. As such this arrangement permits testing to at least 1400^{o}C which is quite adequate for the needs of the project.

To obtain weight changes as a function of time a Cahn 1000 balance was purchased and was incorporated into the experimental arrangement. Finally, in respect to the apparatus, a computer set-up capable of handling the weight changes and a printer were assembled with the balance.

Oxidation Experiments

A relatiavely wide variety of oxidation tests were conducted on iron-based, cobalt-based and nickel-based alloys.

Typical of the iron-based results are those given in Appendix A which is a revised paper that has been submitted for publication in an AIME Symposium - "Alternate Alloying For Environmental Resistance". Basically, these tests were

conducted on alloys with various concentrations of the alloying elements chromium and/or silicon in the iron matrix with variable additions of Si_3N_4 particles. The Si_3N_4 particles dissolved to a major extent in the matrix material and also reacted with any oxygen present. Thus, the final alloy composition was iron + various levels of chromium + silicon at a number of levels + particles of unreacted Si_3N_4 and SiO_2.

Kinetic studies were made at a number of temperatures at about 1 atm of dry oxygen. It was found that the rates of oxidation were extremely slow and were comparable to many of the slowest growing commercial alloys. Optical microscopy, SEM and Kevex studies were also conducted on these alloys prior to and following the oxidation experiments. These studies revealed that the introduction of Si_3N_4 particles and their subsequent reaction with the matrix phase resulted in: (1) a lowering of the chromium content necessary to form a protective Cr_2O_3 layer; (2) altering diffusion in the protective layer(s) from primarily cationic to primarily anionic; (3) decreasing considerably the initial, non-parabolic weight gain; (4) decreasing the grain size of the growing scale; and, (5) the formation of a SiO_2 layer beneath the Cr_2O_3 layer.

Nickel and cobalt based alloys were also tested with additions of Si_3N_4 particles and were found to behave in a manner quite similar to that of the iron based alloys described above.

A small number of oxidation tests at 1000°C with P_{O_2} = 1 atm, were also made with additions of SiAlON, a high temperature compound found in the Si-Al-O-N system, to cobalt-chromium alloys. The particular SiAlON used in these studies was formed by sintering mixtures of Si_3N_4 (85 w/o), Al_2O_3 (10 w/o) and Y_2O_3 (5 w/o) at 1800°C in a nitrogen atmosphere. The Y_2O_3 is added to the SiAlON to aid densification during the sintering process.

The results obtained utilizing 10 v/o and 15 v/o of SiAlON are depicted in Figs. 1 and 2, respectively. Fig. 3 displays the weight gains per unit area of Co-Cr alloys at the same temperature and P_{O_2} as that employed for the alloys with SiAlON additions. In comparing the results depicted in these figures it is seen that the particles and their dissolution products produce protective scales at concentrations of chromium between 10 to 12 wt%. Additionally, the weight gain per unit area for the better alloys containing SiAlON are significantly lower than those found in the binary Co-Cr system. Further work is underway on these alloys. In particular, scales developed and the alloy microstructures must be investigated.

The oxidation behavior of Ni-Cr-SiO_2 alloys has also been investigated. Apendix B is a copy of a paper that will be presented at the Univ. of Keele, England during the week of 1-5 Sept. 1986 at the Fourth International Conference on "Transport In Non-Stoichometric Compounds". Papers given at this meeting will be reviewed for publication in "Advances in Ceramics".

As may be seen from the contents of this paper the levels of concentrations of the dispersed phase SiO_2 were relatively high compared to most studies utilizing dispersions. In addition the size of the particles employed were extremely fine. The results obtained were quite encouraging in that the rates of oxidation were reduced considerably by the introduction of the SiO_2 particles while the chromium contents were at levels considerably less than conventional alloys.

A by-product of the use of high concentrations of a dispersed phase such as SiO_2 in these alloys is the decreased density of the alloy. Utilization of such alloys in systems where weight is important may well be considered as alternatives to conventional alloys.

The final effort described in this report relates to the electrical short circuiting of SiO_2 layers growing on Si (or SiC or Si_3N_4). The initial thought on this aspect was to utilize a noble metal as a wire embedded in the substrate to be oxidized. Unfortunately, essentially all the noble meals react with Si to form silicides or low melting eutectics. A search was and is being made of oxides as possible probes. Such an oxide must not oxidize, must not react with either Si or SiO_2 and should show appreciable electronic conductivity. At this point it appears that Nb_2O_5 may be suitable as a non-interacting short circuiting probe.

Keywords: Thermogravimetric analysis; Microscopy

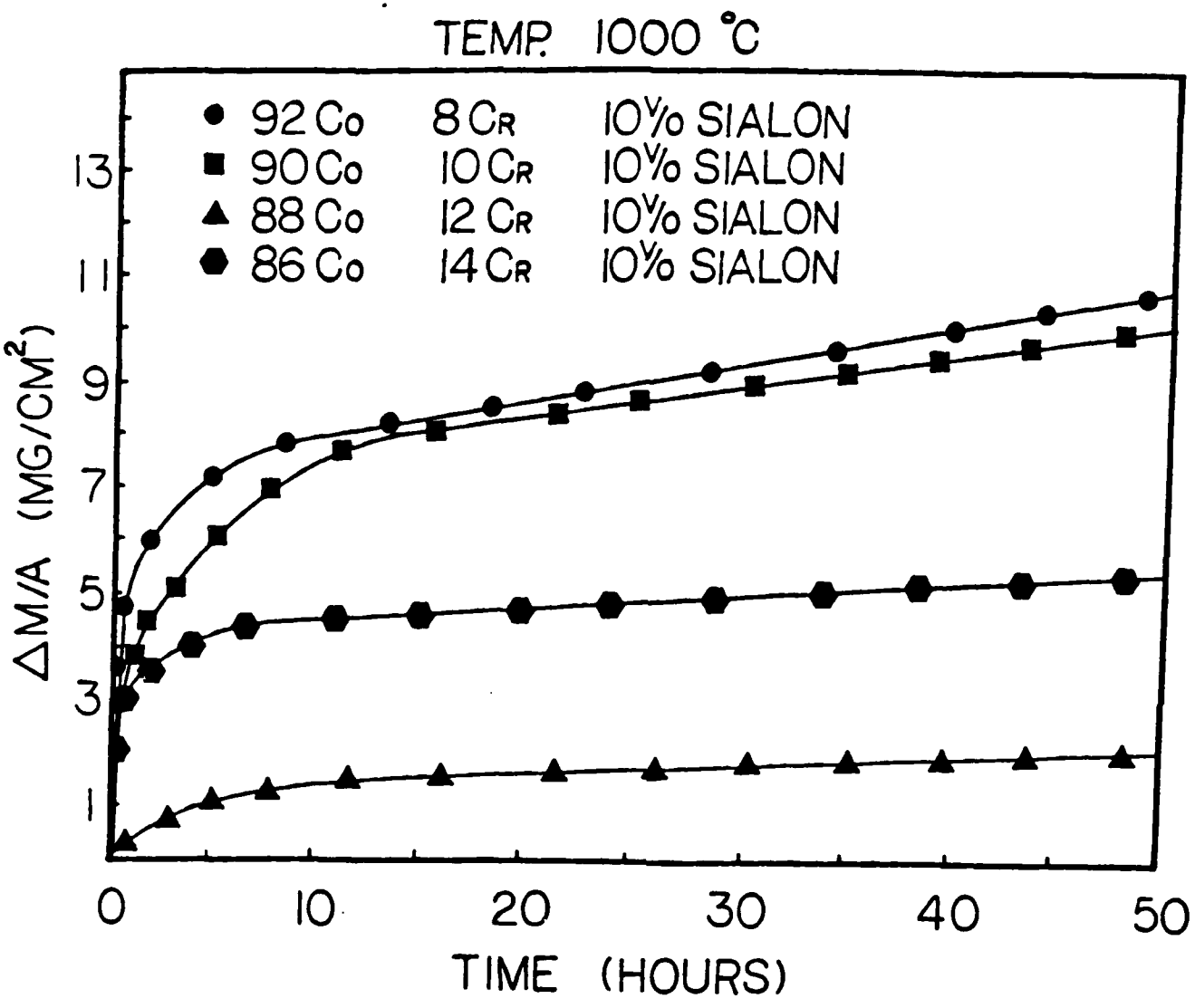

Figure 1. Isothermal oxidation curves for Co-Cr alloys with 10 vol. % SiAlON at 1000 C in 1 atm. O_2.

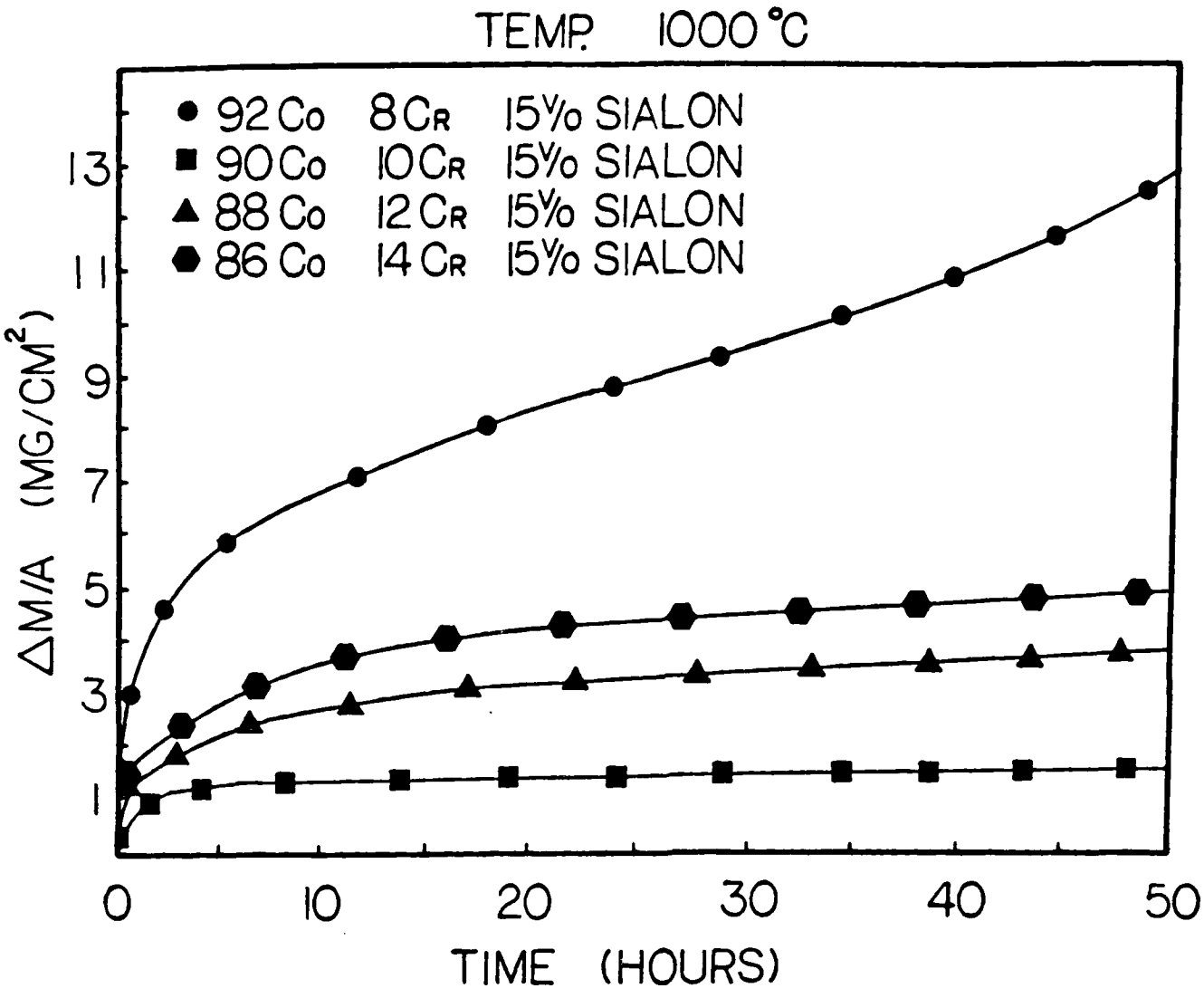

Figure 2. Isothermal oxidation curves for Co-Cr alloys with 15 vol. % SiAlON at 1000 C in 1 atm. O_2.

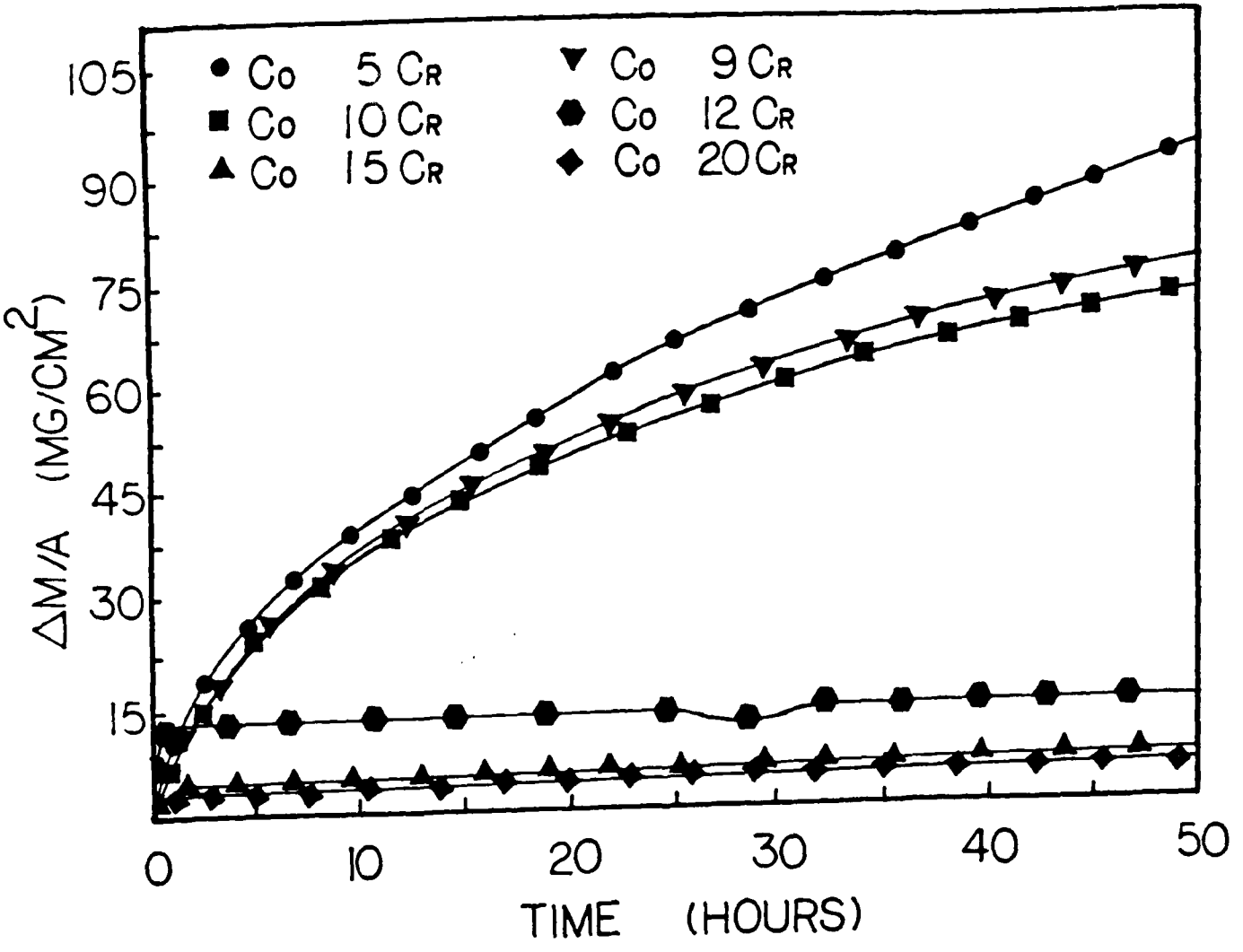

Figure 3. Isothermal oxidation curves for binary Co-Cr alloys at 1000 C in 1 atm. O_2.

APPENDIX A

"HIGH TEMPERATURE OXIDATION OF IRON BASED ALLOYS"

S-W Park and G. Simkovich

Metallurgy Program, Steidle Building
Department of Materials Science and Engineering
The Pennsylvania State University
University Park, PA 16802

Abstract

Iron-chromium alloys (0 to 14wt%Cr) with and without 10 vol % of Si_3N_4 particles, which were unstable in the matrix phase, were oxidized at 1173K and 1273K in 1 atm of oxygen. Oxidation of the iron-chromium alloys without the presence of Si_3N_4 revealed the following. The rate of oxidation decreased as the concentration of chromium was increased. An increase in temperature produced an increase in oxidation rate. Only pure iron showed FeO as a phase along with Fe_3O_4 and Fe_2O_3. As chromium was introduced a chromium spinel appeared as a product along with Cr_2O_3, Fe_3O_4 and Fe_2O_3. At higher chromium concentrations Fe_3O_4 was eliminated as a detectable product. Voids were present at the scale-alloy interface with Pt markers indicating considerable outward diffusion of cations during scale growth.

The initial addition of 10 vol % Si_3N_4, which dissolved extensively in the matrix phase, reduced considerably the rate of oxidation as compared to the nitride free materials. The appearance of an almost complete protective layer of Cr_2O_3 occurred at a quite low chromium concentration, about 5 wt %. Beneath the Cr_2O_3 layer SiO_2 formed to serve in further reducing the rates. It was found that the oxidation rate was relatively insensitive to temperature and that the scale was adherent during temperature cycling. Marker positions following oxidation of these alloys were at the gas - scale interface indicating inward diffusion of oxygen as the primary mode of transport during scale growth.

Revised prior to review and re-submitted for publication in TMS-AIME Symposium on "Alternate Alloying For Environmental Resistance"

Introduction

For high temperature oxidation resistance, a large number of iron based alloys, usually with high chromium contents, have been utilized to develop protective oxide scales. Systematic oxidation studies have been performed in some detail on the oxidation behaviour of binary Fe-Cr alloys(1-3). The oxidation rate of Fe-Cr alloys is reduced as chromium contents in the alloys are increased until about 20 weight percent after which the rate is not changed significantly with increased Cr content. The protective oxide scale formed on most binary Fe-Cr alloys are known to have, in general, poor scale adhesion to the underlying alloys probably due to void formation at the interface between oxide and alloy (4). It has been known that the presence of small amounts of oxides or nitrides such as ThO_2, Y_2O_3, or TiN in Ni-Cr and Fe-Cr alloys affects extensively the oxidation behaviour of such alloys (5-12). The oxidation rate is considerably decreased for alloys containing oxide or nitride dispersions and, additionally, scale adhesion to the underlying alloys is much improved. On the other hand, it is found that 1.29 weight percent of Li_2O in Ni-20Cr (7) and 1 percent SiO_2, TiO_2 or Cr_2O_3 in an Fe-20Cr alloys (6) have either little effect on the oxidation behaviour or increases the oxidation rates. Michels (7) has shown that increasing the amount of Y_2O_3 in Ni-20Cr alloys seems to increase the oxidation resistance although this author was not too concerned with such effects. A number of investigators have proposed several different kinds of models to explain the effects of oxide or nitride dispersions on oxidation behaviour (5-7) even though none of those proposed models have been well accepted as yet. There have been limited studies of the effects of stable oxide or nitride dispersions on iron based chromium containing alloys (6,9). Most of the previous studies have been limited to alloys with high chromium contents (14-20 weight %).

In the present investigation 10 vol% Si_3N_4 was added, prior to sintering, to a variety of Fe-Cr and Fe-Cr-Si alloys. The initial thought concerning this study was to have a silicon source in the Si_3N_4 particles available for growth of a protective scale of SiO_2. However, thermodynamic considerations indicated that a major portion, if not all, of the Si_3N_4 decomposes at the sintering temperature to give an Fe-Cr-Si alloy with some nitrogen in solution. SEM studies, Figure 1, revealed that some Si_3N_4 particles remained after sintering indicating that dissolution did not reach equilibrium. Although the Si_3N_4 particles are unstable in the matrix the oxidation tests proved to be very interesting and are discussed in the following sections.

Thermodynamics of Fe-Si System

The activity of silicon in the Si_3N_4 at 1500K, the sintering temperature in this study, is obtained from the free energy of formation of α-Si_3N_4 (13) assuming that P_{N_2} = 1 atm in this sintering operation. Thus, from

$$Si_{(s)} + 2/3\ N_{2(g)} = 1/3\ Si_3N_{4(s)} \text{ and } \Delta G^o = 389{,}100 + 198T(J) \qquad (1)$$

one obtains $a_{Si} = 6.204 \times 10^{-4}$ at 1500K. At equilibrium the activity in the alloy must equal the activity in the Si_3N_4. Use of the relation

$$\ln \gamma_{Si} = \ln \gamma^o_{Si} + \epsilon^{Si}_{Si} \cdot N_{Si} \qquad (2)$$

where ϵ^{Si}_{Si} is Wagner's self-interaction coefficient and literature values (14) of γ^o (= 3.00×10^{-4}) and ϵ^{Si}_{Si} (= 14) at 1500K gives the relation

Figure 1. Fracture surface topography of Fe-9Cr with an initial addition of 10% Si_3N_4 (≙ 2.89 Si) after sintering for 120 hours at 1500K; note remaining Si_3N_4 particles. A = Si_3N_4 particles B = matrix.

$$\ln \gamma_{Si} = -8.113 + 14\, N_{Si} \qquad (3)$$

Utilizing

$$a_{Si} = \gamma_{Si} \cdot N_{Si} = 6.20 \times 10^{-4} \qquad (4)$$

and solving eqs. (3) and (4) for N_{Si} gives $N_{Si} = 0.176$ in the alloy phase in equilibrium with α-Si_3N_4. Assuming that all the silicon from 10 vol% Si_3N_4 in an Fe-9Cr alloy dissolves into the alloy one obtains $N_{Si} = 0.055$. This is considerably below the value in equilibrium with Si_3N_4 indicating that the particles of Si_3N_4 should dissolve into the alloy for all the cases in this study.

The above analysis ignores the effects of chromium and nitrogen upon the activity of silicon. However, this is justified because ε_{Si}^{Cr} is relatively small (15) and because the concentration of nitrogen in the alloy is probably limited. Both chromium and nitrogen will tend to increase the activity of silicon in the alloy so that the mole fraction value of silicon calculated is probably somewhat greater than the actual equilibrium mole fraction.

Experimental

A series of alloys with and without an initial addition of 10 vol% Si_3N_4 were made by conventional powder metallurgy methods. The starting materials were -100 mesh iron powder, -325 mesh chromium and silicon powder and α-Si_3N_4 whose particle size ranges between 0.01 μm to 1 μm. The composition of the materials are listed in Table 1. The powders were mixed thoroughly, cold-pressed and then reduced at 1273K for 6 hours followed by a sinter at about 1500K in evacuated vycor or silica tubes for 96 to 120 hours. Alloys of Fe-Cr-Si were prepared in a similar fashion. The sintered samples were air quenched and were prepared for oxidation by grinding through 600 grit SiC abrasive paper and then were carefully washed and rinsed wih acetone. Isothermal oxidation behaviour was measured by weight gain vs. time in about 1 atm of flowing oxygen on disc specimens approximately 1.2 cm in diameter x 0.2 cm in thickness. The samples were suspended with Pt wire from one arm of an automatic recording semi-micro balance (Ainsworth) in a Vycor reaction tube. Isothermal tests at 1173 and 1273K were conducted up to 80 hrs. When the oxidation test was started,

the sample was exposed to flowing oxygen and the test temperature was attained in about 3 min. No corrections for loss of weight due to nitrogen release was made since only a small amount of Si_3N_4 particles remained after sintering and were involved in the actual oxidation reaction.

Table 1 - Composition of the materials

Materials	C	O	Cl	S	Mo	Si	Fe	Si_3N_4
A1000B	0.015			0.016		0.01	Balance	
Si_3N_4*		0.087	0.04		0.0097			
Cr	99.97% purity							

* α content = 92.7%

Table 2 lists some of the alloys tested with additions of 10 vol% Si_3N_4. The resulting alloy compositions assuming that all of the Si_3N_4 dissolved into the matrix alloy are also listed. It is noted that the silicon content of such alloys is between 2.85 and 2.90 wt% Si.

Table 2 - The Concentration of Silicon in Alloys Assuming Complete Dissolution of the Initial Addition of Si_3N_4 Particles

Alloy Composition	Total Silicon Content	
wt%	wt% Si	Mole Fraction Silicon
Fe-10 vol% Si_3N_4	2.84	0.055
Fe-3Cr-10 vol% Si_3N_4	2.85	0.055
Fe-5Cr-10 vol% Si_3N_4	2.88	0.055
Fe-7Cr-10 vol% Si_3N_4	2.88	0.055
Fe-9Cr-10 vol% Si_3N_4	2.89	0.056
Fe-14Cr-10 vol% Si_3N_4	2.90	0.056
Fe-3Cr-2Si-10 vol% Si_3N_4	4.86	0.092
Fe-9Cr-2Si-10 vol% Si_3N_4	4.87	0.092
Fe-3Cr-1Si	1.00	0.020
Fe-3Cr-2Si	2.00	0.039
Fe-3Cr-3Si	3.00	0.058
Fe-9Cr-1Si	1.00	0.020
Fe-9Cr-2Si	2.00	0.039
Fe-9Cr-3Si	3.00	0.058

Upon the completion of kinetic measurements, the oxidized specimen was examined to evaluate surface topography by using the scanning electron microscope. Transverse sections of representative specimens were prepared by standard metallographic techniques and examined by optical microscopy and scanning electron microscopy. Some of the oxidized specimens were examined with a kevex-ray to evaluate the qualitative analysis of element distribution in the oxide scale. Standard x-ray diffraction techniques

were also employed for phase identification of the scales. Some of oxidized alloys which initially contained Si_3N_4 were heated after vacuum encapsulation in SiO_2 tubes at 1573 K and then held for 6 hours in order to transform the amorphous SiO_2 formed at the reaction temperature to a crystalline SiO_2 phase (cristobalite). Platinum marker experiments were conducted on Fe-9Cr alloys with and without 10 vol % Si_3N_4 to compare he oxide growth mechanisms on these alloys at 1273 K under 1 atm O_2.

Results

Oxidation Kinetics

Typical oxidation curves on Fe-Cr alloys, including pure Fe, with and without an initial 10 vol % Si_3N_4 (≙ 2.84 to 2.90 wt% Si), are plotted in Figures 2 to 5 as weight gain, in mg/cm^2, vs time, in hours, at 1173 K and 1273 K under 1 atm O_2. Figure 2 shows that the addition of Si_3N_4 reduces the oxidation rates significantly in comparison to that of pure Fe.

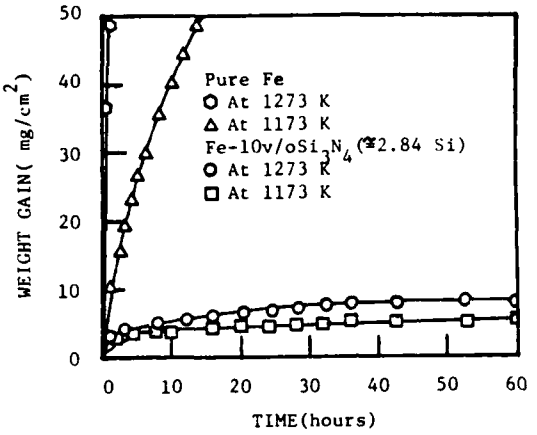

Figure 2. Isothermal oxidation curves for pure Fe with and without an initial addition of 10% Si_3N_4 (≙ 2.84 Si) at 1173 and 1273 K.

Similar behaviour is observed on the series of Fe-Cr alloys with again an initial 10 vol% Si_3N_4 (Figures 3 and 4). The incorporated Si_3N_4 reduces not only the oxidation rate but also the weight gain during the initial oxidation period even in an alloy containing only 3 weight percent of chromium. From these plots, it is seen that the major portion of the weight gain on all the Fe-Cr alloys with Si_3N_4 is essentially completed within the initial 20 hours of the oxidation period and also the oxidation rate is decreased with time, showing that a protective oxide scale forms. In addition, the oxidation behaviour of Fe-Cr alloys with Si_3N_4 additions exhibits little temperature dependence unlike that of the binary Fe-Cr alloys. Figure 5 shows the oxidation behaviour of the Fe-Cr alloys with an initial 10 vol% Si_3N_4 as a function of chromium content at 1273 K. A significant reduction in initial weight gain, which is completed within the initial 20 hours of oxidation, is seen as the chromium content in the alloys is increased until about 9 weight percent of chromium after which there is an increase in weight gain. Figure 6 shows two different weight gains, one after the first 20 hours and the other after 60 hours, plotted as a function of chromium content in the alloys containing initially Si_3N_4. From this plot, little difference between the two different weight gains is observed. This indicates that the formation of the protective scale is virtually completed within 20 hours in the Fe-Cr alloys with the introduction of silicon via the Si_3N_4 particles and in the presence of the un-reacted nitride particles.

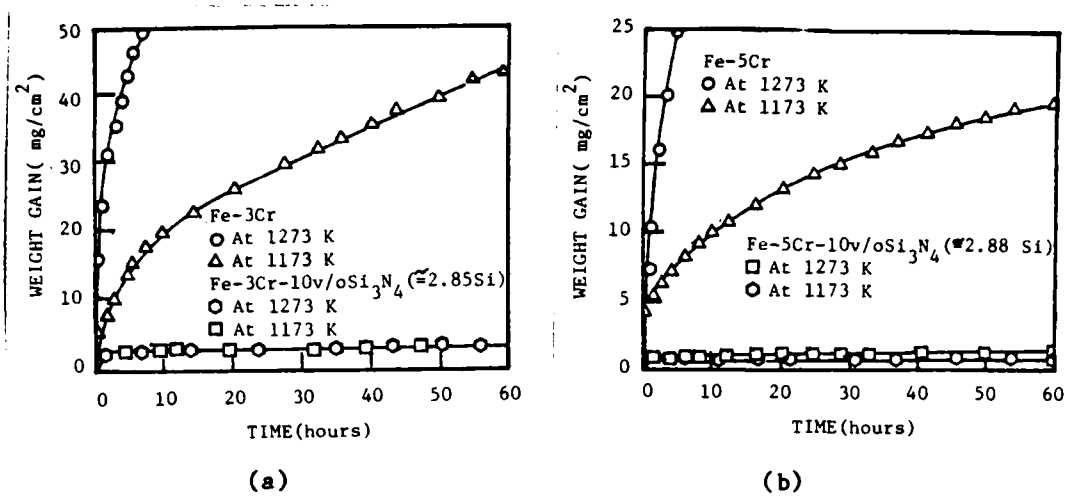

Figure 3. Isothermal oxidation curves a) for Fe-3Cr alloys with and without and initial addition of 10 v/o Si_3N_4 (= 2.85 Si), b) for Fe-5Cr alloys with and without an initial addition of 10 v/o Si_3N_4 (= 2.88Si) in 1 atm O_2 at 1173K and 1273K.

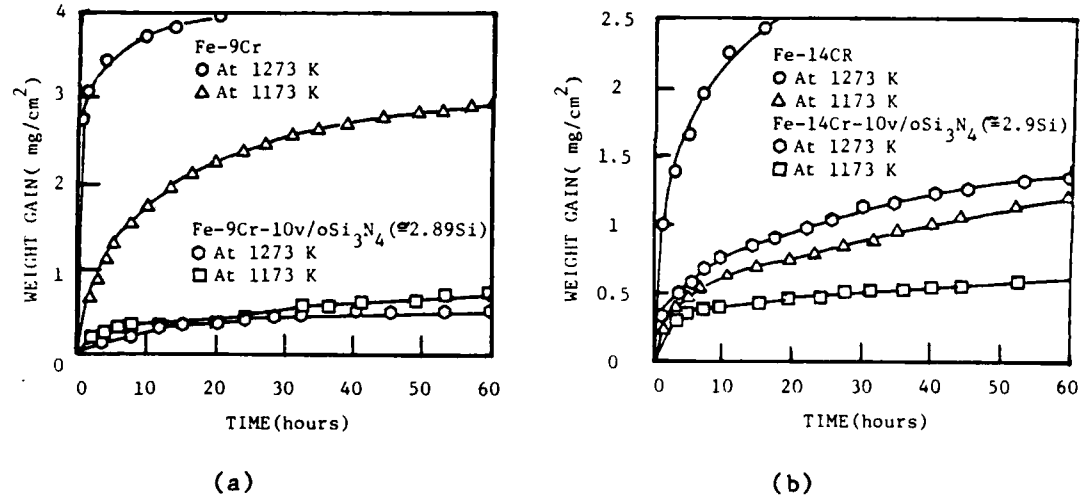

Figure 4. Isothermal oxidation curves a) for Fe-9Cr alloys with and without an initial addition of 10 v/o Si_3N_4 (=2.89 Si), b) for Fe-14Cr alloys with and without an initial addition of 10 v/o Si_3N_4 (=2.90 Si).

A number of runs were also made on Fe-Cr-Si alloys. From plots of $(\Delta m/A)^2$ vs. time parabolic rate constants were calculated for these alloys and a few of the alloys containing the 10 vol% Si_3N_4 addition. The alloys and the derived parabolic rate constants are listed in Table 3. A number of factors are evident from the values listed in Table 3. Among these are the following. (1) Introduction of silicon directly to an Fe-Cr alloy decreases considerably the parabolic rate constants, except for the slightly anomalous behavior of the Fe-9Cr-1Si alloy. (2) The use of Si_3N_4 as a source of silicon dramatically reduces the parabolic rate constants of alloys of comparable silicon and low chromium contents. Thus, the effects produced by the use of Si_3N_4 particles are not fully explained by the resulting silicon contents indicating that the un-reacted particles and other factors may well effect the kinetics of reaction.

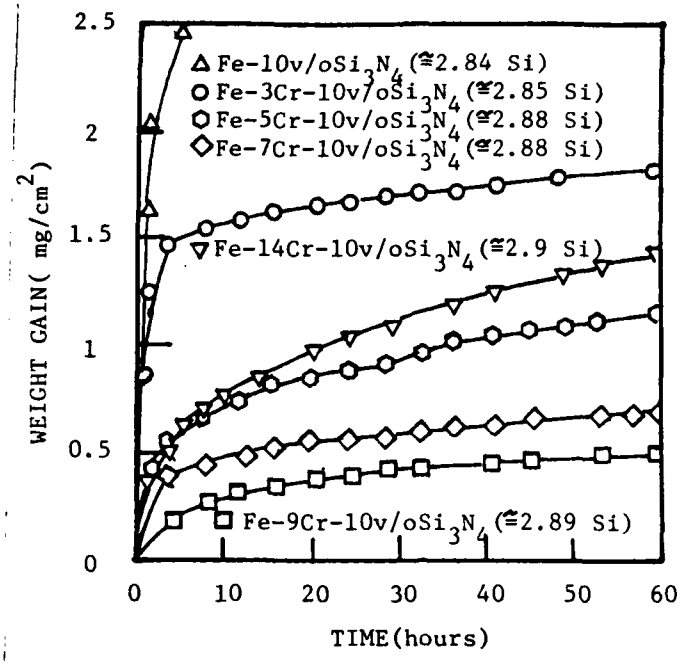

Figure 5. Isothermal oxidation curves for Fe-Cr alloys with an initial addition of 10 v/o Si_3N_4 as a function of Cr content in 1 atm O_2 at 1273 K.

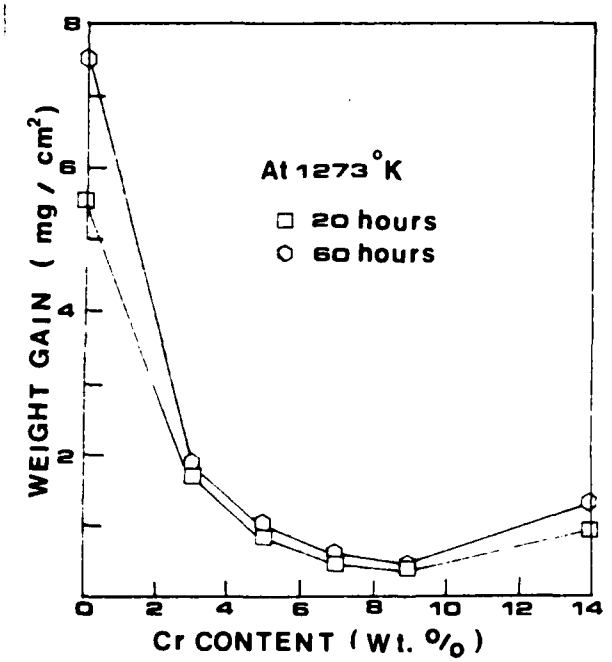

Figure 6. Weight gain in Fe-Cr alloys with an initial addition of 10 v/o Si_3N_4 (see Table 2); one for initial 20 hours and the other for 60 hours in 1 atm O_2 at 1273 K.

Table 3 - Parabolic Rate Constants of Various Iron Based Alloys at 1273K - P_{O_2} ≅ 1 atm.

Iron-Based Alloy Composition wt%	Parabolic Constants $g^2cm^{-4}sec^{-1} \times 10^{14}$
Fe-3Cr	1,300,000.
Fe-3Cr-1Si	750,000.
Fe-3Cr-2Si	1,100.
Fe-3Cr-3Si	730.
Fe-3Cr-10 vol% Si_3N_4 (≅ 2.85 Si)	3.3
Fe-3Cr-2Si-10 vol% Si_3N_4 (Σ ≅ 4.86 Si)	0.55
Fe-9Cr	82,000.
Fe-9Cr-1Si	220,000.
Fe-9Cr-2Si	850.
Fe-9Cr-3Si	63.
Fe-9Cr-10 vol% Si_3N_4 (≅ 2.89 Si)	0.56
Fe-9Cr-2Si-10 vol% Si_3N_4 (≅ 4.87 Si)	290.

Morphology

Figure 7 shows the typical surface topography of pure iron, with and without the initial Si_3N_4 addition, after 50 hrs of oxidation at 1273 K. Fairly fine oxide grains and a smooth oxide surface are obtained on pure Fe with Si_3N_4 with a few oxide nodules, which are found in limited areas, while large oxide grains are observed on pure iron. Figure 7(c) and (d) show in more detail the oxidized surface of pure Fe with initial additions of Si_3N_4. There are only limited areas in which iron oxide overgrows the protective scale. Cross sections of regions of pure Fe, are seen in Figure 8. The thickness of oxide scale formed on pure Fe with initial additions of Si_3N_4 is significantly reduced while the thickness of oxide scale formed on pure Fe is considerable (several hundreds μm). Also, the oxide scale formed on pure Fe with Si_3N_4 is dense and has no void formation at the interface between metals and oxide. During cooling, after completing the kinetic measurement, neither significant spalling nor crack propagation of oxide is observed in pure Fe to which Si_3N_4 was added prior to sintering.

Figure 9 shows the surface topography of Fe-5Cr alloys, with and without initital Si_3N_4 additions, after 68 hours of oxidation at 1273 K. There is a significant difference between the oxide formed on these alloys. On the Fe-5Cr with the initial Si_3N_4 particles, the localized iron oxide occurs in limited areas only and the remaining portion of the surface is covered with a fine chromium oxide while on the Fe-5Cr alloy without Si_3N_4 only iron oxide is observed. The iron oxide formed on Fe-5Cr with the initial Si_3N_4 addition is localized to a few oxide nodules (Figure 9(b)). The cross sections of Fe-3Cr and Fe-5Cr alloys with the initial 10 vol% Si_3N_4 are shown in Figure 10. A thin and dense oxide scale, with some oxide nodules, is formed and pegged into the metal matrix without an internal oxidation zone.

Figure 11 shows the surface topography of Fe-9Cr with Si_3N_4 oxidized at 1173 K. The oxide over the entire region of the surface of the Fe-9Cr alloy with Si_3N_4 consists of essentially pure Cr_2O_3 while only iron oxide is formed on the surface of the Fe-9Cr alloy. It appears that the surface

oxide grooves on the chromium oxide lie parallel to the grinding grooves resulting from sample preparation. Similar features are observed in Fe-14Cr with an initial 10 vol% Si_3N_4 addition.

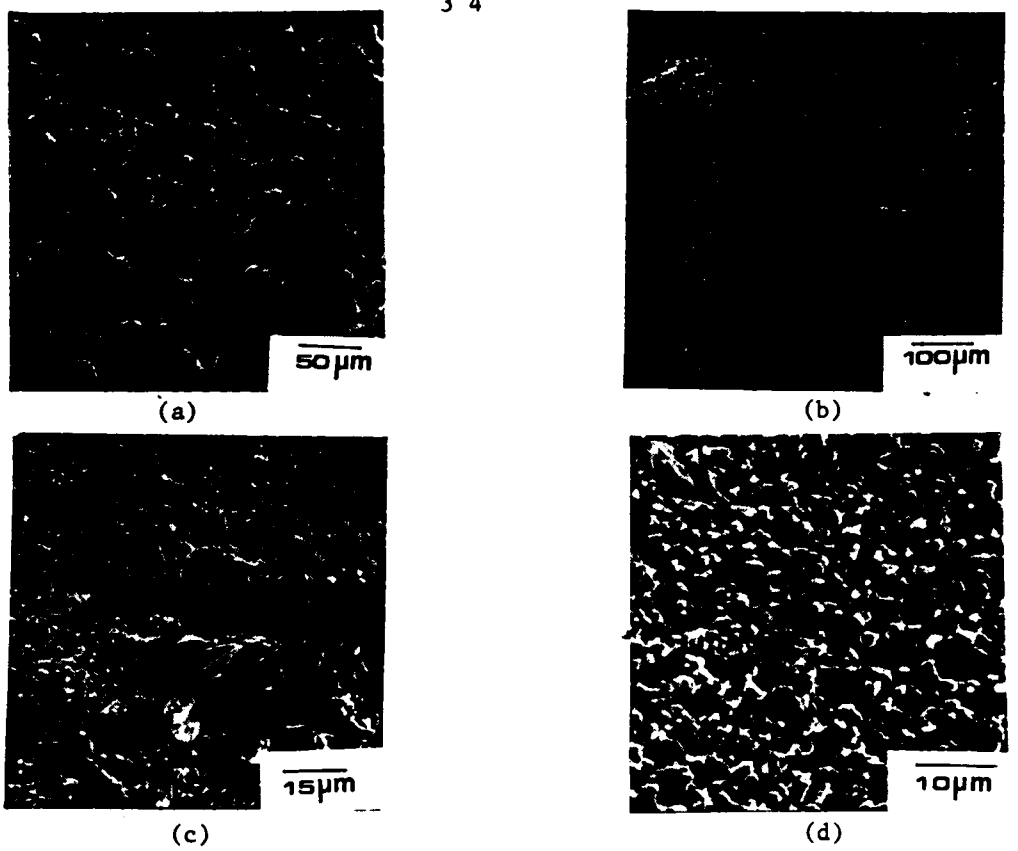

Figure 7. (a) Surface topography of pure Fe after 50 hours of oxidation at 1273 K; note the large iron oxide grains.

(b) Surface topography of Fe with an initial addition of 10 v/o Si_3N_4 (≡2.284 Si) after 50 hours oxidation at 1273 K; a smooth iron oxide surface with oxide nodules.

(c) and (d) detailed view of (b): Showing (c) over-grown oxide and (d) fairly fine oxide grains.

Figure 12 shows the cross section of Fe-9Cr alloys oxidized for 50 hours at 1273 K. The internal oxidation zone with a thick external oxide scale is obvious in the binary Fe-9Cr alloy while thin and complex oxide scales are formed on the Fe-9Cr alloy with an initial 10 vol% Si_3N_4 additive. Figure 13(b) shows the concentration profile of elements in B area and Figure 13(c) in A area in Figure 13(a). These indicate that area B consists of essentially pure Cr_2O_3 while area A is primarily SiO_2.

Figure 14(b), shows that platinum markers initially placed on the alloy surface prior to oxidation are found on the top of the Cr_2O_3 formed on an Fe-9Cr alloy with Si_3N_4 after 50 hours of oxidation at 1273 K and the underlying Cr_2O_3 is seen in Fig. 14(a). On the other hand, the platinum marker is found in the middle of the oxide scale formed on an Fe-9Cr alloy

without Si_3N_4 after 72 hours oxidation at 1273°K (Figure 14(c)). This difference in marker position shows the change of oxide growth mechanism due to the incorporated silicon and remaining Si_3N_4 particles.

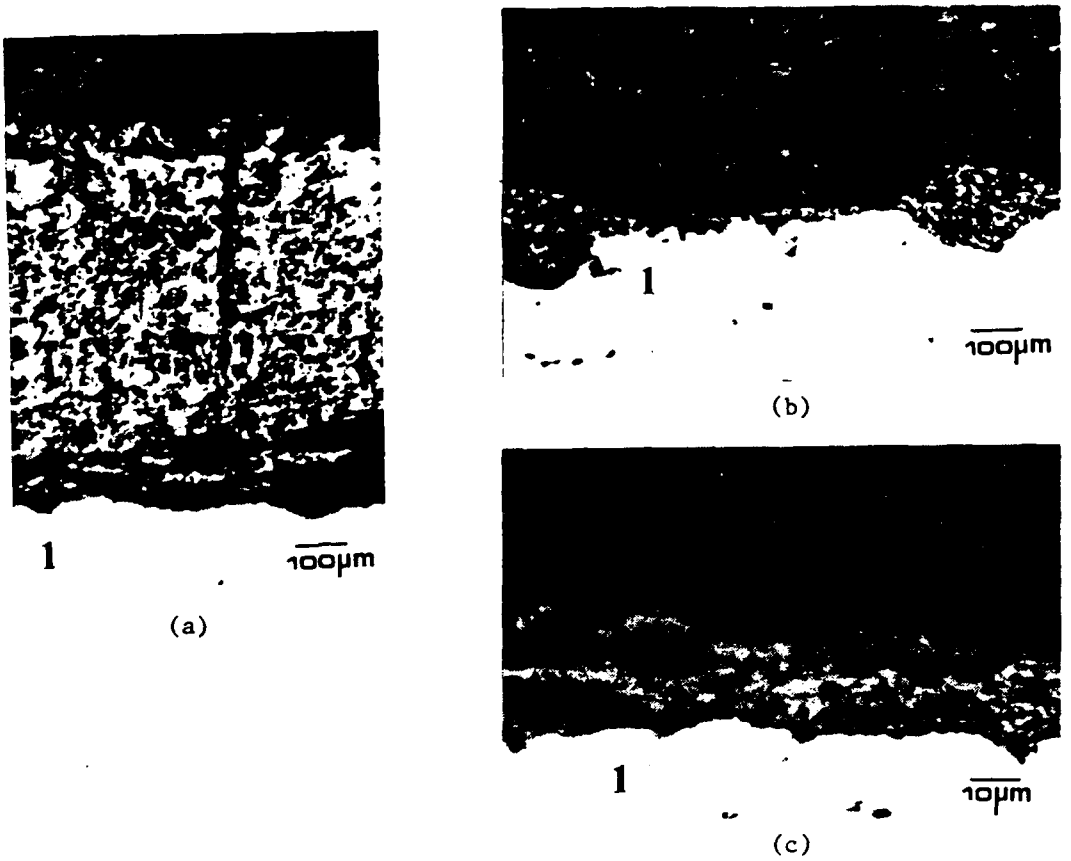

Figure 8. (a) Cross section of pure Fe after 50 hours oxidation at 1273 K; showing thick and porous iron oxide scale.

(b) Cross section of pure Fe with an initial addition of 10 v/o Si_3N_4 after 50 hours oxidation at 1273 K; showing relatively thick oxide nodule with thin oxide scale.

(c) detailed view of (b): the formed oxide scale in dense and pore free at the interface between metal and oxide

1: matrix 2: oxide scale 3: mounting material

It is noted that the figures presented in this section do not reveal the presence of any particles of Si_3N_4 remaining following the oxidation process. However, Figure 1 does show some nitride particles and additionally dissolution in acids of the alloys did give a residue whose x-ray patterns confirmed to α-Si_3N_4. Thus, the effects observed in these alloys must relate to both the silicon in the alloy as well as the un-reacted Si_3N_4 particles. The data in Table 3 already indicates that such must be the case.

X-ray Diffraction

Phase identification of the oxide scale was determined by X-ray diffraction analysis utilizing diffractometer and Debye-Sherrer

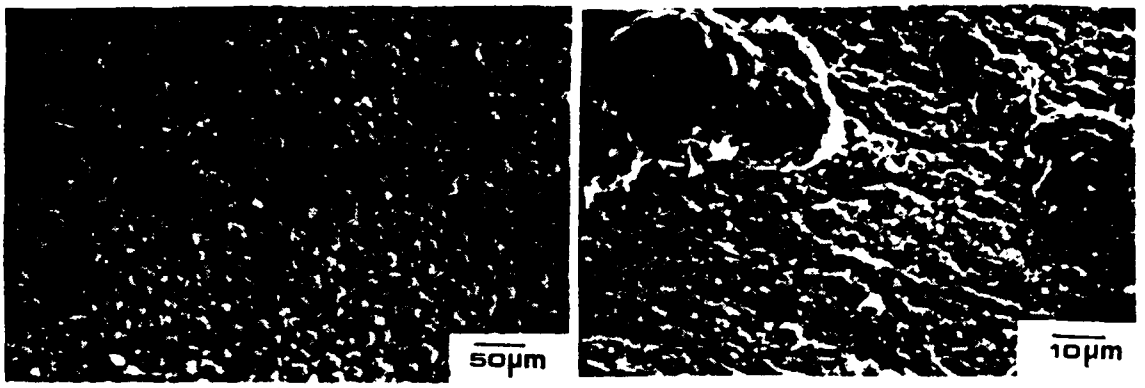

Figure 9. Surface topography of Fe-5Cr alloys (a) without and (b) with an initial addition of 10 v/o Si_3N_4 (≅2.88Si) after 68 hours oxidation in 1 atm O_2 at 1273 K
1: Fe_2O_3 2. Cr_2O_3 3: Cr_2O_3/Fe_2O_3

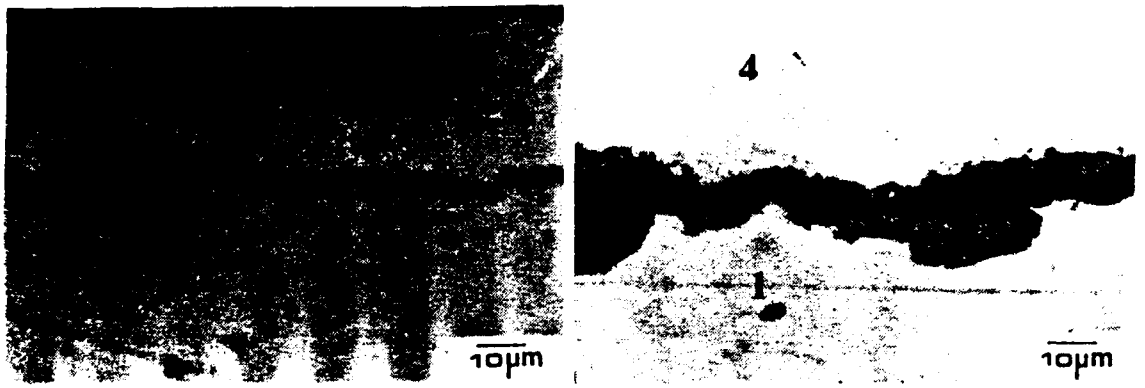

Figure 10. Cross section of (a) Fe-3Cr alloy with an initial addition of 10 v/o Si_3N_4 (≅2.85Si) after 60 hours oxidation (b) Fe-5Cr alloy with an initial addition of 10 v/o Si_3N_4 (≅2.88Si) after 68 hours oxidation in 1 atm O_2 at 1273 K
1: matrix 2: SiO_2 scale 3. Fe_2O_3 formed as oxide nodule
4: electroplated Ni coating.

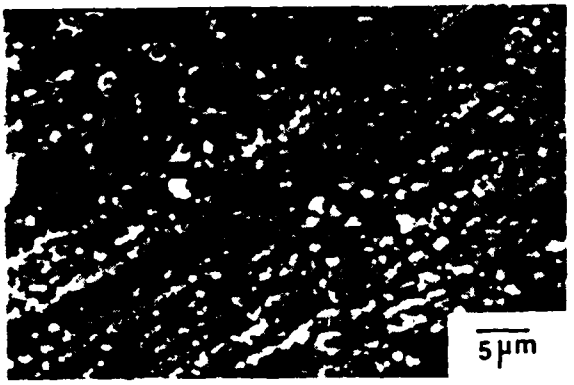

Figure 11. Surface topography of Fe-9Cr alloy with an initial addition of 10 v/o Si_3N_4 (≅2.89Si) after 70 hours oxidation at 1173 K showing the surface oxide grooves on the chromium oxide.

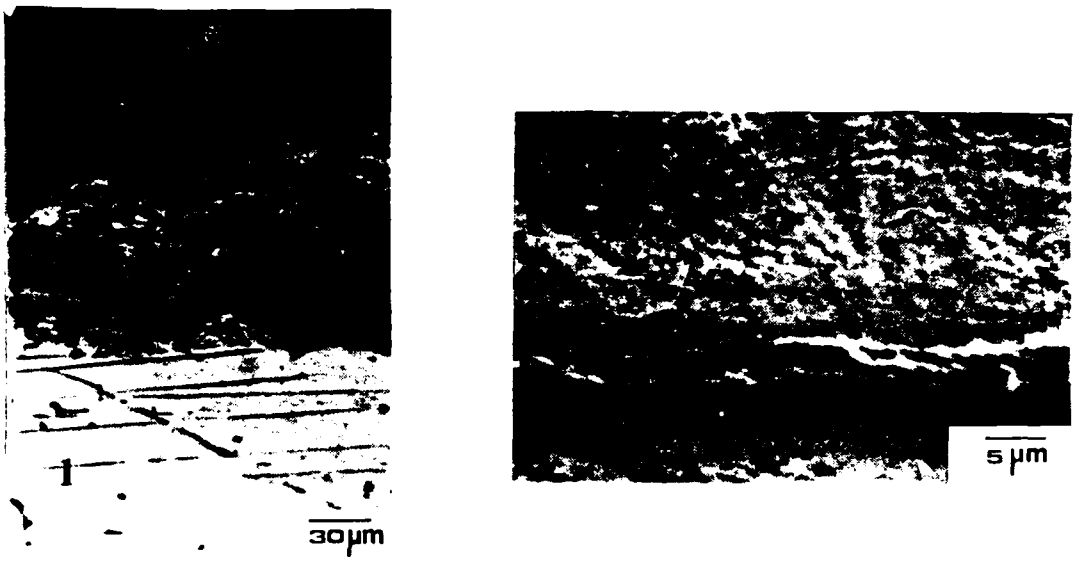

(a) (b)

Figure 12. Cross section of (a) Fe-9Cr alloy after 48 hours oxidation at 1273 K (b) Fe-9Cr alloy with an initial addition of 10 v/o Si_3N_4 (≙2.89Si) after 50 hours oxidation at 1273 K.
1: matrix 2. Internal oxidation region 3: oxide scale
4: mounting material 5: electroplated Ni coating.

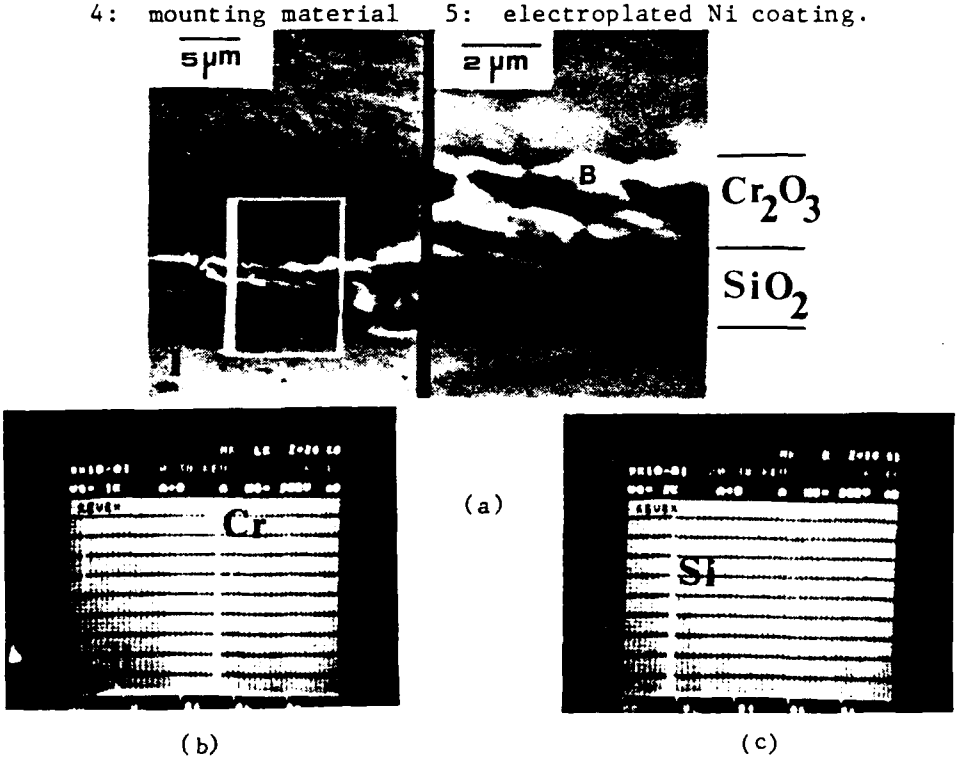

(a)

(b) (c)

Figure 13. (a) Cross section of Fe-9Cr with an initial addition of 10 v/o Si_3N_4 (≙2.89Si) after 50 hours oxidation at 1273K, (b) Concentration profile of elements in B showing high concentration of Cr; (c) Concentration profile of elements in area A showing high concentration of Si. 1: matrix, 2: oxide scale, 3: electroplated Ni coating.

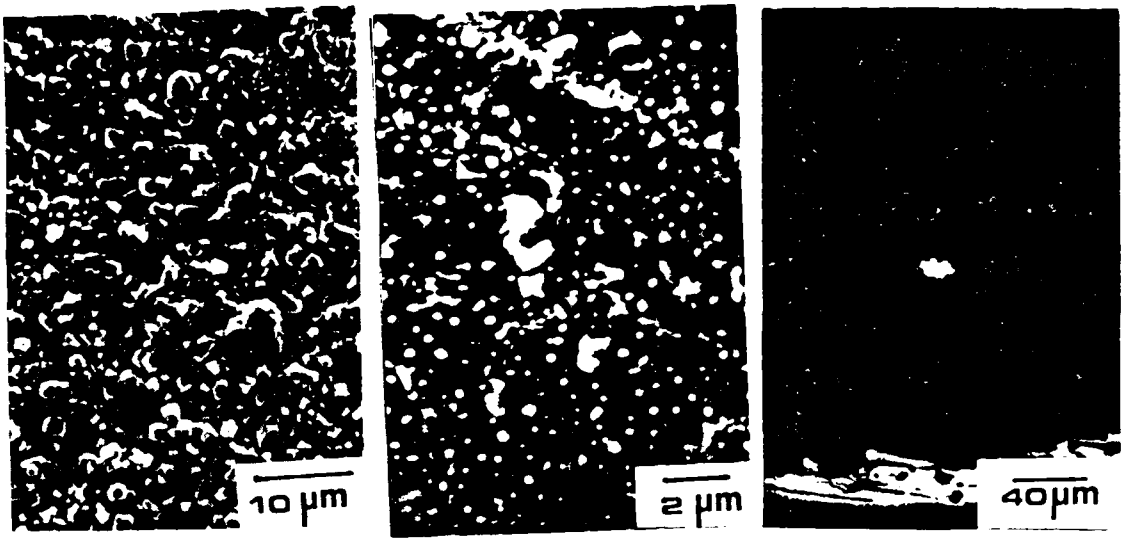

(a) (b) (c)

Figure 14. (a) Fine chromium oxide on surface of Fe-9Cr with an initial addition of 10 v/o Si_3N_4 (≅2.89Si) after 50 hours of oxidation at 1273 K
(b) Pt markers on top of the chromium oxide formed on Fe-9Cr with an initial addition of 10 v/o Si_3N_4 (≅2.89Si) at 1273 K
(c) Pt marker in the middle of the oxide scale formed on Fe-9Cr alloy without Si_3N_4 at 1273 K.

techniques. Samples to be X-rayed were enclosed in evacuated SiO_2 tubes and held for 6 hours at 1573 K to crystallize the SiO_2 portion of the scale. After cooling, some of the oxide was detached, which was determined to be Cr_2O_3 and Fe_2O_3 and the adhering oxides were determined to be SiO_2 with some Cr_2O_3. The oxides in Fe-Cr alloys with initial Si_3N_4 additions consisted of Fe_2O_3, Cr_2O_3 and SiO_2. The amounts of Fe_2O_3 decreased as the chromium content in the alloys was increased until no Fe_2O_3 was detected in the Fe-9Cr with Si_3N_4. In pure Fe with an initial addition of 10 vol% Si_3N_4, only Fe_2O_3 was detected. On the other hand, the oxides in binary Fe-Cr alloys without Si_3N_4 consisted of Fe_2O_3, Fe_3O_4, Cr_2O_3 and some $Fe_2Cr_2O_4$. FeO was not found in Fe-Cr alloys except for pure Fe. As the chromium content was increased, the ratio of Fe_2O_3/Fe_3O_4 increased and, in the Fe-14Cr, no Fe_3O_4 was detected in this study.

Discussion

For Fe-Cr alloys (including pure Fe) with an initial addition of 10 vol% Si_3N_4 the oxidation results show that the incorporated Si_3N_4 reduces the oxidation rate compared to binary Fe-Cr alloys without Si_3N_4 additions over the entire range of chromium content 1173 K and 1273 K under 1 atm O_2 (Figures 1 to 3).

In pure iron, the reduced oxidation rate appears to be due to the formation of SiO_2, resulting from the oxidation of the silicon and the Si_3N_4 particles since there is apparently a low iron diffusivity through the SiO_2 oxide scale. Further details of the formation of the SiO_2 layer will be discussed subsequently. A relatively thin oxide scale is formed with some thick oxide nodules in limited areas at 1273 K. These thick oxide nodules are not found at 1173 K. The thick oxide nodules might be formed due to the break away of the formed SiO_2 (16). Except for the oxide

nodules, it is found that the oxide scale formed is dense, particularly at the interface between metal and oxide, in pure Fe with an initial addition of Si_3N_4 while very porous oxide is formed with void formation at the interface in pure Fe. Also, the grain size of oxide on the surface of pure Fe with additions of 10 vol% Si_3N_4 is much reduced even in the oxide nodules. The difference between the formed oxide with and without Si_3N_4 particle additions may be due to the change of the oxidation mechanism.

In the Fe-Cr alloys with initial Si_3N_4 additions similar results are observed in oxidation behaviour. In particular, it is found that an external, continuous Cr_2O_3 layer is developed on the Fe-Cr alloys with Si_3N_4 additions instead of an external iron oxide in binary Fe-Cr alloys not containing Si_3N_4. Very thin and fine grained Cr_2O_3 scale, with isolated oxide nodules, is formed on Fe-3Cr and Fe-5Cr alloys with initial Si_3N_4 additions. Those isolated oxide nodules do not form on Fe-9Cr and 14 Cr alloys with the Si_3N_4 additions. In previous investigations (8,9), it was reported that the presence of small amounts of stable oxide or nitride dispersions appears to reduce the critical bulk concentration of chromium in Fe and Ni based Cr containing alloys necessary to form a continuous, external Cr_2O_3 layer during oxidation. However, the previous investigations were limited to Ni and Fe base alloys with high chromium content (14-20 weight %). However, in the present investigation, the results indicate that the critical bulk concentration of chromium necessary to form an external continuous Cr_2O_3 layer is significantly reduced by incorporating silicon via large amounts of particles of Si_3N_4 in alloys prior to sintering.

This may be a result of increased nucleation of Cr_2O_3 on the remaining Si_3N_4 particles (or formed SiO_2) which produces a fine grained Cr_2O_3 through which motion of Fe is slow and under which SiO_2 layers may form to provide additional oxidation resistance. Stringer (9) has shown similarly that fine grained Cr_2O_3 forms on alloys containing oxide dispersions.

From the oxidation curves in Figure 2 to 5 it is seen that, in most of the Fe-Cr alloys with Si_3N_4, the oxidation rates are decreased with time, showing that the oxide scales have protective properties. This is due to the formation of protective Cr_2O_3/SiO_2 layers resulting from oxidation of the Cr containing alloy and the incorporated silicon and the remaining Si_3N_4. The protective properties of the SiO_2 scale in the Fe-Cr alloys with Si_3N_4 might be explained by the model of blocking layers of stable oxides in oxide scales (5,17). However, such is not the case in our alloys since most of our added particles reacted upon sintering to produce alloys containing silicon in solid solution with minor amounts of un-reacted Si_3N_4 particles. Nevertheless, these complex alloys do change the pattern of growth (Figure 13) from predominantly outward ion motion to anion motion inward. Such results from the silicon available to form an almost complete SiO_2 layer underlying the Cr_2O_3 layer (Figure 12).

The variation of chromium content in the Fe-Cr alloys containing initial additions Si_3N_4 greatly effects the oxidation behaviour. These results are illustrated in Figure 5. The initial weight gain is greatly reduced as the chromium content is increased while, after the initial oxidation period, the variation of chromium content in the alloy with initial Si_3N_4 additions does not materially effect further oxygen up-take (Figure 6). The reduction in the weight gain during the initial oxidation period is also due to the early appearance of external chromium oxide, which also leads to the reduction of the amount of iron oxide formed.

Acknowledgements

We extend sincere thanks to The Pennsylvania Research Corporation, the Metallurgy Program at Penn State and the Air Force Office of Scientific Research (Grant No. 85-0298) for their kind support of this study.

Reference

1. D. Mortimer and W. B. A. Sharp, "Oxidation of Fe-Cr Binary Alloys," British Corrosion Journal, 3(2) 1968, 61-67.
2. D. Lai, R. J. Borg, M. J. Bruler, J. D. Mackenzie and C. E. Birchenall, "Oxidation of Iron-Chromium Alloys at 750-1025°C," Corrosion, 17 (1961), 357t-364t.
3. I. G. Wright, "Oxidation of Iron-, Nickel-, and Cobalt-Base Alloys," (Report MCIC-72-07, Metals and Ceramics Information Center, 1972).
4. V. R. Howes, "Metal-Oxide Interface Morphology for a Range of Fe-Cr Alloys," Corrosion Science, 10 (1970), 99-103.
5. C. S. Giggins and F. S. Pettit, "The Oxidation of TD NiC (Ni-20Cr-2 vol pct ThO_2) Between 900° and 1200°C," Metallurgical Transactions, 2 (1971), 1071-1078.
6. H. Nagai, Y. Takebayashi and H. Mitami, "Effect of Dispersed Oxides of Rare Earth and Other Reactive Elements on the High Temperature Oxidation Resistance of Fe-20Cr Alloy," Metallurgical Transactions A, 12A (1981), 435-442.
7. H. T. Michels, "The Effect of Dispersed Reactive Metal Oxides on the Oxidation Resistance of Nickel - 20 wt % Pct Chromium Alloys," Metallurgical Transactions A, 7A (1976), 379-388.
8. M. S. Seltzer, B. A. Wilcox and J. Stringer, "The Oxidation Behavior of Ni-Cr-Al-2ThO_2 Alloys at 1093 and 1204°C," Metallurgical Transactions, 3 (1972), 2391-2401.
9. O. T. Goncel, J. Stringer and D. P. Whittle, "The Effect of Internal Stable Nitride and Oxide Dispersion on the High Temperature Oxidation of Fe-Cr Alloys," Corrosion Science, 18 (1978), 701-719.
10. J. Stringer, B. A. Wilcox, and R. I. Jaffee, "The High-Temperature Oxidation of Nickel-20 wt % Chromium Alloys Containing Dispersed Oxide Phases," Oxidation of Metals, 5 (1) (1972), 11-47.
11. H. H. Davis, H. C. Graham, and I. A. Kvernes, "Oxidation Behaviour of Ni-Cr-1ThO_2 Alloys at 1000 and 1200°C," Oxidation of Metals, 3 (5) (1971), 229-241.
12. G. R. Wallwork and A. Z. Hed, "The Oxidation of Ni-20 wt % Cr - 2ThO_2," Oxidation of Metals, 3 (3) (1971), 229-241.
13. A. Hendry, "Thermodynamics of Silicon Nitride and Oxynitride", in Nitrogen Ceramics, ed. by F. L. Riley, Noordhoff Inter Publishing, Reading, Mass., U.S.A. 183-185 (1977).
14. H. Sakao and J. F. Elliott, "Thermodynamics of Dilute bcc Fe-Si Alloys", Metallurgical Transactions A, 6A (1975) 1849-1851.
15. T. Fujisawa, S. Kimura and H. Sakao, "Effects of Vanadium, Chromium, Molybdenum and Wolfram on the Activity of Silicon in Solid Iron", Tetsu-to-Hagane, 67 (1981) 940-945.
16. R. L. Logan and W. w. Smeltzer, "The Growth of Wustite-Fayallite Nodules on an Iron - 1.5 wt % Silicon Alloy Exposed to Carbon Dioxide - Carbon Monoxide Atmospheres," Oxidation of Metals, 3 (3) (1971), 279-290.
17. R. A. Meussner and C. E. Birchenall, "The Growth of Ferrous Sulfide on Iron," Corrosion, 13 (1957), 677t-689t.

APPENDIX B

High Temperature Oxidation of Ni-Cr Alloys Containing a Dispersed Phase

S-W. Park and G. Simkovich

Metallurgy Program, Steidle Building
Department of Materials Science and Engineering
The Pennsylvania State University
University Park, PA 16802

ABSTRACT

The oxidation behavior of Ni-Cr alloys (0-15 wt% Cr) with and without SiO_2 particles as a dispersion, whose amounts were varied from 5 to 40 volume percent, was studied at 1173K to 1373K in 1 atm of oxygen. The presence of SiO_2 as a dispersion in Ni-Cr alloys reduced considerably the oxidation rate as compared to the binary Ni-Cr alloys whereas the SiO_2 particles incorporated into pure Ni showed little effect on oxidation behavior. The oxidation rate of Ni-Cr alloys with SiO_2 particles as a dispersion phase showed a strong dependence on the inter-relation between volume percent of SiO_2 incorporated and chromium contents ion the Ni-Cr alloys. The critical bulk concentration of chromium in the Ni-Cr alloys necessary to form an external, continuous Cr_2O_3 layer was significntly reduced by adding SiO_2 as a disperson to the alloys. For Ni-Cr alloys containing SiO_2 particles, inward diffusion of oxygen ions was deduced to be responsible for oxide growth.

Introduction

Systematic oxidation studies have been well documented for binary Ni-Cr alloys, including pure Ni[1-7]. Small additions of Cr to Ni increase the oxidation rate. The maximum oxidation rate is obtained at about 3~5 wt% Cr. With an increase in Cr content the oxidation rate then decreases due to Cr_2O_3 and $NiCr_2O_4$ blocking effects. Chromium additions of about 20 weight percent markedly reduce the oxidation rate due to formation of a continuous Cr_2O_3 scale underneath an external NiO scale. Thus, for high temperature oxidation resistance, a large number of Ni based alloys, usually with about 20 weight percent of chromium contents, have been utilized to develop protective oxide scales.

It has been known that the presence of small amounts of oxides or nitrides such as ThO_2, Y_2O_3, TiO_2 or TiN in Ni-Cr, Co-Cr and Fe-Cr alloys affects markedly the oxidation behavior of such alloys[8-14]. The oxidation rate is considerably decreased for alloys containing oxides or nitrides and, additionally, scale adhesion to the underlying alloys is much improved. On the other hand, it is found that the addition of small amounts of Li_2O or La_2O_3 in Ni-20Cr alloys[10] and SiO_2, Al_2O_3 and Cr_2O_3 in Fe-20Cr alloys[9] show either little effect on oxidation behavior or increased the oxidation rates. A number of investigators have proposed several different kinds of models to explain the effects of oxide or nitride dispersions on high temperature oxidation behavior[8-11] although none of those proposed models have been universally accepted. Most of the previous studies have been limited to alloys with high chromium contents (14-20 weight percent) and with small amounts of an incorporated dispersion (2-5 volume percent).

In the present investigation, the effects of SiO_2 as a dispersed phase on the oxidation behavior of a number of Ni-Cr alloys are studied. There are three

distinctive approaches that differ from previous investigations: first, chromium contents in the Ni-Cr alloy with SiO_2 as a dispersion are varied, from 0 to 15 wt% Cr, to evaluate chromium content effects; secondly, unusually large amounts of SiO_2 particles are incorporated for the specific purpose of forming continuous protective SiO_2 scales; and, finally, the amount of SiO_2 as a dispersion incorporated into the Ni-Cr alloys is varied to evaluate the inter-relation between effects of chromium contents and volume percent of SiO_2 on the oxidation behavior.

Experimental

A series of alloys, with and without additions of SiO_2, were made by conventional powder metallurgy methods. The starting materials were 2~3 μm Ni powder, (99% purity), 2 μm chromium and amorphous SiO_2 (fumed silica) whose individual particle size ranges between 30 to 300 Å. The powders were mixed thoroughly, using a high speed blender and ball mill, and then were cold pressed. The cold pressed specimens were reduced in H_2 at 1273K for 6 hours followed by sintering at 1500K in evacuated vycor or silica tubes for 100 hours. The microstructures of a Ni-9Cr alloy, with and without 20 v/o SiO_2 particles, are shown in Fig. 1. The average grain size of Ni-9Cr alloys are shown in Figure 2 as a function of volume percent of incorporated SiO_2 particles. It appears that the grain size of the Ni-9Cr alloys with SiO_2 as a dispersion is significantly reduced as the volume percent of SiO_2 incorporated into the alloys is increased. The initially added amorphous SiO_2 was transformed to crystalline SiO_2 (cristobalite), which was detected by x-ray diffraction analysis, during the sintering procedure. The sintered samples were air quenched and were prepared for isothermal oxidation tests by grinding to 600 grit on silicon carbide abrasive paper and then were carefully washed and rinsed with acetone.

Isothermal oxidation behavior was measured by weight gain vs. time in about 1 atm of slow flowing oxygen on disc specimens 1.2 cm in diameter and 0.2 cm in thickness. The samples were suspended with Pt wire from one arm of an automatic recording semi-micro balance in a vycor reaction tube. Isothermal tests at 1173K, 1273K and 1373K were conducted up to 60 hours. When the oxidation test was started, the sample was exposed to flowing oxygen and heated to the test temperature in about 3 min. The weight gain measurements were not corrected for the formation of a gas phase resulting from the oxidation of Cr_2O_3 to gaseous CrO_3.

Upon completion of the kinetic measurement, the oxidized specimen was examined by scanning electron microsopy to evaluate surface topography. Transverse sections of representative specimens were prepared by standard metallographic techniques and examined by optical microscopy and scanning electron microscopy. Some of the oxidized specimens were examined with energy dispersive x-ray spectroscopy (E.D.S.) to evaluate elemental distribution in the oxide scale. Standard x-ray diffraction techniques were also employed for phase identification of the scales.

Results

Oxidation Kinetics

Typical oxidation curves on Ni-Cr alloys, including pure Ni, with and without SiO_2 dispersed particles, are plotted in Figures 3 to 7 as weight gain (mg/cm^2) versus time (hours) at 1173K to 1373K in 1 atm O_2. In Figure 3, the weight changes of pure Ni and Ni-3Cr alloys, with and without incorporated SiO_2 particles, at 1273K are shown. The addition of SiO_2 in pure Ni increased the initial oxidation rate after which the oxidation rates become quite similar during the steady state oxidation periods. Increased amounts of SiO_2 show

almost negligible effects on the oxidation behavior. On the other hand, the incorporated SiO_2 in Ni-3Cr alloys slightly reduces the oxidation rates both in the initial and the steady state periods of oxidation. The oxidation resistance is increased as the volume percent of SiO_2 in Ni-3Cr alloys is increased.

The effects, significant, of incorporated SiO_2 on the oxidation resistance of Ni-9Cr alloys are shown in Figure 4. The 5 volume percent of SiO_2 in the Ni-9Cr alloys increased the initial oxidation rates at 1273K and 1373K. After short periods of time, the oxidation rate is significantly reduced. Such seems to be due to the completion of a protective scale. Further addition of SiO_2 particles in the Ni-9Cr alloys reduced the oxidation rates systematically. As shown in Figure 4(b), sizable weight losses are obtained for Ni-9Cr alloys containing 10, 20 and 40 volume percent of SiO_2 during oxidation at 1373K. Similar oxidation behavior is observed for both Ni-12Cr and Ni-15Cr alloys with SiO_2 as a dispersion, Figures 5 and 6. Again, weight losses are observed in all of the alloys containing SiO_2 as a dispersion during oxidation at 1373K. Such loss of weight is apparently due to the formation of the volatile oxide CrO_3.

The weight changes obtained during oxidation of Ni-9Cr alloys with 10 and 20 volume percent of SiO_2 are plotted against time for temperatures from 1173K to 1373K in Figure 7. The initial weight gains of all of the alloys are decreased as the temperature is decreased. Furthermore, the differences in weight changes between Ni-9Cr-10 v/o SiO_2 and Ni-9Cr-20 v/o SiO_2 are significantly increased as the test temperature is increased.

In Figures 8a and 8b, the oxidation behavior of Ni-Cr alloys containing 20 volume percent of SiO_2 is replotted as a function of chromium contents at 1273K and 1373K respectively. The oxidation rates are dramatically reduced as the chromium contents are increased to 9 weight percent at 1273K. Further increase in the chromium content shows negligible effects on the oxidation behavior at

1273K. Similar behavior is obtained at 1373K but at a higher chromium content (12 weight percent).

Morphology

The surface topography of pure Ni, with and without SiO_2 particle additions, after 50 hours of oxidation at 1273K, is shown in Figure 9. Smaller grains of NiO for Ni-20 v/o SiO_2 in comparison to pure Ni are observed. Cross sections of pure Ni, with and without SiO_2, are shown in Figure 10. The oxide formed on Ni with 20 volume percent of SiO_2 are pegged into the metal matrix while the oxide formed on pure Ni shows a smooth interface.

A significant difference between the oxide topography on Ni-9Cr alloys, with and without 20 volume percent of SiO_2 addition, after 54 hours oxidation at 1273K, is shown in Figure 11. The oxide over the entire region of the surface of the Ni-9Cr-20 v/o SiO_2 alloy is primarily Cr_2O_3, while only NiO oxide is formed on the surface of the Ni-9Cr alloy. The surface topography of the Ni-9Cr-20 v/o SiO_2 alloy; after 64 hours oxidation at 1373K, is shown in Figure 12. The development of relatively large oxide nodules, which are mainly Cr_2O_3 and small amounts of NiO_2, are shown in Figure 12(a). The appearance of SiO_2 particles on the oxide surface are shown in Figure 12(b). Similar topographies of oxide surfaces are developed on the Ni-12Cr and Ni-15Cr alloy containing SiO_2. The cross sections of Ni-9Cr alloys, with and without SiO_2, oxidized for 60 hours at 1373K are shown in Figure 13. A thick and smooth oxide scale, mainly NiO, is formed on the Ni-9Cr alloy while a thin and complex oxide scale develops on the Ni-9Cr alloy with SiO_2. This latter scale is pegged into the metal matrix which additionally does not display an internal oxidation zone. Similar oxide scales are formed on the Ni-15Cr-10 v/o SiO_2 as shown in Figure 14.

The cross section of a Ni-12Cr alloy with 40 volume percent of SiO_2, oxidized for 60 hours at 1373K, is shown in Figure 15(a). Again a thin and complex oxide scale is developed. It is noted that SiO_2 particles are found in the Cr_2O_3 oxide, which is confirmed by the E.D.S. spectrum for Areas A shown in Figure 15(b). In Figure 15(b) and 15(c), the E.D.S. spectrums for Areas B and C are shown. From these spectrums one concludes that the main oxides formed on the Ni-9Cr-40 v/o SiO_2 are Cr_2O_3 and SiO_2.

X-ray Diffraction

Phase identification of the oxides formed during oxidation was determined by x-ray diffraction analysis utilizing diffractometer and Debye-Sherrer techniques. The oxides in Ni-Cr alloys consist of NiO and $NiCr_2O_4$ with some Cr_2O_3, which is only detected in the Ni-12Cr and Ni-15Cr alloys. In pure Ni with SiO_2 as a dispersion; the outer oxide scale consists mainly of NiO with some SiO_2 while the inner oxide consists of NiO, SiO_2 and Ni_2SiO_4. For the Ni-3Cr alloy with SiO_2, the outer oxide scale is mainly NiO and the inner oxide consists of Cr_2O_3, NiO, $NiCr_2O_4$ and SiO_2. Note that no Cr_2O_3 was detected on the binary Ni-3Cr alloy. In this study Cr_2O_3 and SiO_2 were always detected in Ni-Cr alloys containing SiO_2 particles. For Ni-9Cr alloys with SiO_2, the constituents of the oxide scale showed a strong dependency on the volume percent of incorporated SiO_2 and the temperature of oxidation. For Ni-9Cr alloys with low volume percents of SiO_2, x-ray diffraction analysis showed that the oxide scale for Ni-9Cr with SiO_2 consisted of NiO, Cr_2O_3, $NiCr_2O_4$ and SiO_2 (crystobalite) while the oxide scale for the binary Ni-9Cr alloy consisted of NiO and $NiCr_2O_4$. For Ni-9Cr-20 v/o SiO_2 alloy, no NiO was detected at 1273°K but at 1373K a small amount of NiO was found. No NiO was observed for Ni-9Cr with 40 volume percent of SiO_2 at either 1273K or 1373K. For the Ni-12Cr and

15Cr alloys with SiO_2 as a dispersion only Ni-12Cr alloy with 10 volume percent of SiO_2 showed the presence of NiO after oxidation at 1373K. A $NiCr_2O_4$ phase was always detected except for the Ni-12Cr and Ni-15Cr alloys with 40 volume percent of SiO_2.

Discussion

In pure nickel, the addition of SiO_2 as a dispersion does not significantly change the oxidation kinetics. Previous investigations[15,16] on Ni with 2 weight percent of ThO_2 showed similar oxidation behavior except no increase in the initial oxidation rate of the ThO_2 containing alloys occurred. The increased initial oxidation rate in Ni with 10 and 20 volume SiO_2 may be due to the increased reaction areas for the initial oxidation period since the incorporated particles might be simply detached from the matrix during metallographic preparation for the oxidation test resulting from the poor adhesion between the metal matrix and the SiO_2 particles as shown in Figure 1(a). Furthermore the cavities, which were previously occupied by SiO_2 particles, might be underlain by other SiO_2 particles since the distance between the dispered SiO_2 particles is small due to the incorporation of large amounts of SiO_2 into the pure Ni. Additionally, pores formed during sintering might be involved in this increase of initial area. By incorporating large amounts of SiO_2 particles into pure Ni, several effects on oxidation behavior are expected. The incorporated SiO_2 paricles provide more grain boundary area as a result of the reduced grain size. Such boundaries provide a fast path for ion transport. Also, the particles reduce the cross sectional area available for ion transport. According to J. Stringer et al[11], dispersed particles in Ni-Cr alloy eliminate short circuit paths such as dislocations. Such reduces the oxidation rates since short circuit paths provide regions for rapid ion transport. Furthermore, NiO doped

with SiO_2 has an increased cation vacancy concentration, which increases the oxidation rate. However, the oxidation results show little differences between pure Ni with and without additions of SiO_2. In view of the null effect of the SiO_2 particles in pure Ni one can only remark that whatever changes occur in the growth mechanism are such that they basically "balance out" to "no change" in the kinetics.

For Ni-Cr alloys containing SiO_2 as a dispersion, the oxidation results show that the presence of dispersed SiO_2 particles reduces the oxidation rate compared to binary Ni-Cr alloys over the entire range of chromium contents at temperatures from 1173K to 1373K (Figures 3 to 6). In Ni-3Cr alloys, the oxidation rates are gradually decreased as the volume percent of SiO_2 is increased. This seems to be due mainly to the formation of Cr_2O_3/SiO_2 particles, which act as barriers for ion transport. However, a continuous Cr_2O_3 scale or SiO_2 layer was not found as an inner oxide layer. It should be noted again that no Cr_2O_3 was detected after oxidation of the binary Ni-3Cr alloy. The concentration of Cr_2O_3 is increased as the volume percent of SiO_2 in the Ni-3Cr alloys is increased. Previous studies[1,17] have indicated rapid diffusion of chromium along grain boundaries on fine-grained Ni-20Cr alloys. A similar behavior for Cr_2O_3 formed in the Ni-3Cr alloy with SiO_2 as a dispersion might be considered since the incorported SiO_2 in Ni-Cr alloys dramatically decreases the grain size as shown in Figure 2.

The significant effects of incorporated SiO_2 on the oxidation behavior of Ni based alloys containing intermediate amounts of Cr (9-15 weight percent) are shown in Figure 4 to 6. In particular, it is found that an external continuous Cr_2O_3 layer is developed on all of the alloys with additions of SiO_2. The formation of an external continuous Cr_2O_3 scale has a strong relationship to the chromium contents and volume percent of SiO_2 in the Ni-Cr alloys. For Ni-9Cr

alloys with SiO_2, the alloy containing 40 volume percent of SiO_2 did not form NiO at 1373K. For Ni-12Cr alloys only the Ni-12Cr with an addition of 10 volume percent of SiO_2 formed NiO at 1373K. For Ni-15Cr alloys, none of the alloys showed the formation of NiO. On the other hand, spinel oxide ($NiCr_2O_4$) was always found for all of the Ni-Cr alloys with SiO_2 except Ni-12Cr and Ni-15Cr alloys with additions of 40 volume percent of SiO_2. Thus any NiO formed during the early stage of oxidation must eventually become converted to $NiCr_2O_4$ by reaction with Cr_2O_3. In previous studies[11,14], it was reported that the presence of small amounts of stable oxides or nitride dispersions in Ni, Co or Fe based alloys with high chromium contents (16-20 weight %) appears to reduce the critical bulk chromium content necessary to form a continuous external Cr_2O_3 layer during oxidation. However, in the present investigation, the results indicate that the critical bulk concentration of chromium necessary to form an external continuous Cr_2O_3 layer is significantly reduced by incorporating large amounts of SiO_2. This might be explained by an initial selective oxidation of chromium due to rapid diffusion of chromium along grain boundaries since, as shown in Figure 2, the grain size of the alloy containing SiO_2 is dramatically reduced. Fleetwood[18] found that sub-grain boundaries in Ni-20Cr with $2ThO_2$ are rapid diffusion paths for chromium. Additionally, according to Stringer et al[11], stable, fine particles act as nucleation sites for Cr_2O_3 and help to form a continuous Cr_2O_3 layer at early stages of oxidation.

The weight loss shown to occur at 1373K oxidation of Ni-9Cr, Ni-12Cr, and Ni-15Cr alloys containing SiO_2 as a dispersion, Figure 4(b), 5(b), and 6, is due to the evaporation of chromium oxide through the reaction[19,20].

$$Cr_2O_3 \text{ (solid)} + 3/2\ O_2 \text{ (gas)} = 2CrO_3 \text{ (gas)}$$

From the oxidation curves in Figures 4 to 7, it is seen that the oxidation rates of most of the Ni-Cr alloys containing SiO_2 particles are significantly reduced in comparison to the oxidation rates of the binary Ni-Cr alloys. The reduced oxidation rates are due to the formation of a continuous protective Cr_2O_3 layer resulting from selective oxidation of chromium in the alloys. In addition, the SiO_2 particles in the Cr_2O_3 layer, as shown in Figure 15(a), induce a further reduction in oxidation rates by decreasing the cross sectional area of Cr_2O_3 available for the transport of ions for oxidation and, according to J. Stringer and et. al.[11], by blocking the short circuit paths for rapid diffusion of chromium. Birchenall[21] and Giggins and Pettit[8] also suggest that stable oxide dispersions can act as diffusion barriers for outward motion of ions. Therefore, when an oxide grows normally by outward cation diffusion the presence of such stable oxides block the cation motion and inward diffusion of anions will occur. In the present investigation, the presence of the SiO_2 particles in the Cr_2O_3 layer, as shown in Figure 14 and 15, suggests that inward diffusion of oxygen ions (or atoms) is favored since the SiO_2 particles may be considered as inert markers.

Acknowledgements

We extend sincere thanks to the Metallurgy Program at Penn State and the Air Force Office of Scientific Research (Grant No. 85-0298) for their kind support of this study.

References

1. C. S. Giggins and F. H. Pettit, Trans. TMS-AIME, 245, 2495 (1969).

2. D. L. Douglass, Corrosion Sci., 8, 665 (1968).

3. H. V. Atkinson, Oxid. Metals, 24, 177 (1985).

4. I. G. Wright, Report MCIC-72-07, Metals and Ceramics Information Center (1972).

5. G. C. Wood and T. Hodgkiess, Nature, 211, 685 (1966).

6. F. A. Elrefaie, A. Manolesiu and W. W. Smeltzer, J. Electrochem. Soc., 132, 2489 (1985).

7. K. Fueki and J. B. Wagner, Jr., J. Electrochem. Soc., 112, 384 (1965).

8. C. S. Giggins and F. S. Pettit, Met. Trans., 2, 1071 (1971).

9. H. Nagai, Y. Takebayashi and H. Mitami, Met. Trans. A, 12A, 435 (1981).

10. H. T. Michels, Met. Trans. A, 7A, 379 (1976).

11. J. Stringer, B. A. Wilcox and R. I. Jaffee, Oxid. Metals, 5(1), 11 (1972).

12. H. H. Davis, H. C. Graham and I. A. Kvernes, Oxid. Metals, 3(5), 229 (1971).

13. G. R. Wallwork and A. Z. Hed, Oxid. Metals, 3(3), 229 (1971).

14. D. T. Goncel, J. Stringer and D. P. Whittle, Corrosion Sci., 18, 701 (1978).

15. D. A. Jones and R. E. Westerman, Corrosion, 21, 295 (1965).

16. F. S. Pettit and E. J. Felten, J. Electrochem. Soc., 111, 135 (1964).

17. C. S. Giggins and F. S. Pettit, Trans. TMS-AIME, 245, 2509 (1969).

18. M. J. Fleetwood, J. Inst. Metals, 94, 218 (1966).

19. H. C. Graham and H. H. Davis, J. Amer. Ceram. Soc., 54(2), 89 (1971).

20. S. A. Jansen and E. A. Gulbransen, 4th International Congress on Metallic Corrosion, September (1969).

21. R. A. Meussner and L. E. Birchnall, Corrosion, 13, 677t (1957).

LIST OF FIGURES

Figure 12. Surface topography of Ni-9Cr with 20 volume percent of SiO_2 after oxidation at 1373K for 44 hours. (a) large oxide nodule formed on the oxide surface (b) details of (a) SiO_2 particles appear on oxide surface. 1 : Cr_2O_3 2 : Cr_2O_3/NiO 3 : SiO_2.

Figure 13. Cross section of Ni-9Cr alloy (a) with and (b) without 20 volume percent of SiO_2 oxidized at 1273K for 50 hours. 1 : matrix 2 : NiO with $NiCr_2O_4$ 3^2: Cr_2O_3 4 : SrO_2 5 : mounting materials 6 : Bi.

Figure 14. Cross section of Ni-15Cr alloy with 20 volume percent of SiO_2 oxidized at 1273K for 50 hours. 1 : metal matrix 2 : Cr_2O_3 3 : SiO_2 4 : Bi.

Figure 15. (a) Cross section of Ni-12Cr alloy with 40 volume percent of SiO_2 oxidized at 1373K for 60 hours. E.D.S. spectrum for (b) Area A, (c) Area B, (d) Area C. 1 : Metal matrix 2 : Cr_2O_3 3 : SiO_2 4 : Bi.

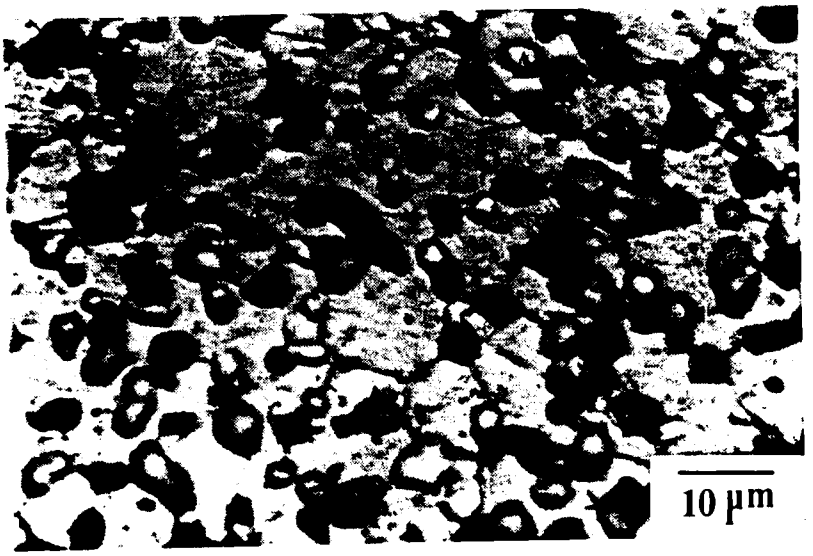

a

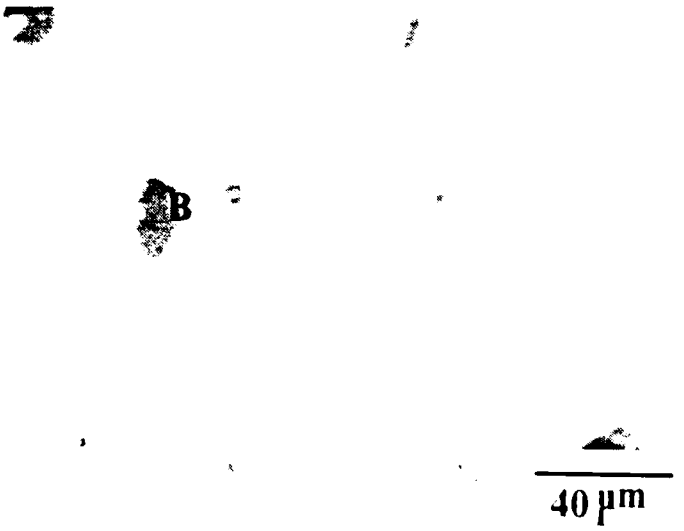

b

Figure 1. Microstructures of Ni-9Cr alloy (a) with and (b) without 20 volume percent of SiO_2 as a dispersion after sintering at 1500K for 100 hours. A : SiO_2 particles in Ni-9Cr alloy with 20 v/o SiO_2. B : pores formed during sintering in the Ni-9Cr alloy.

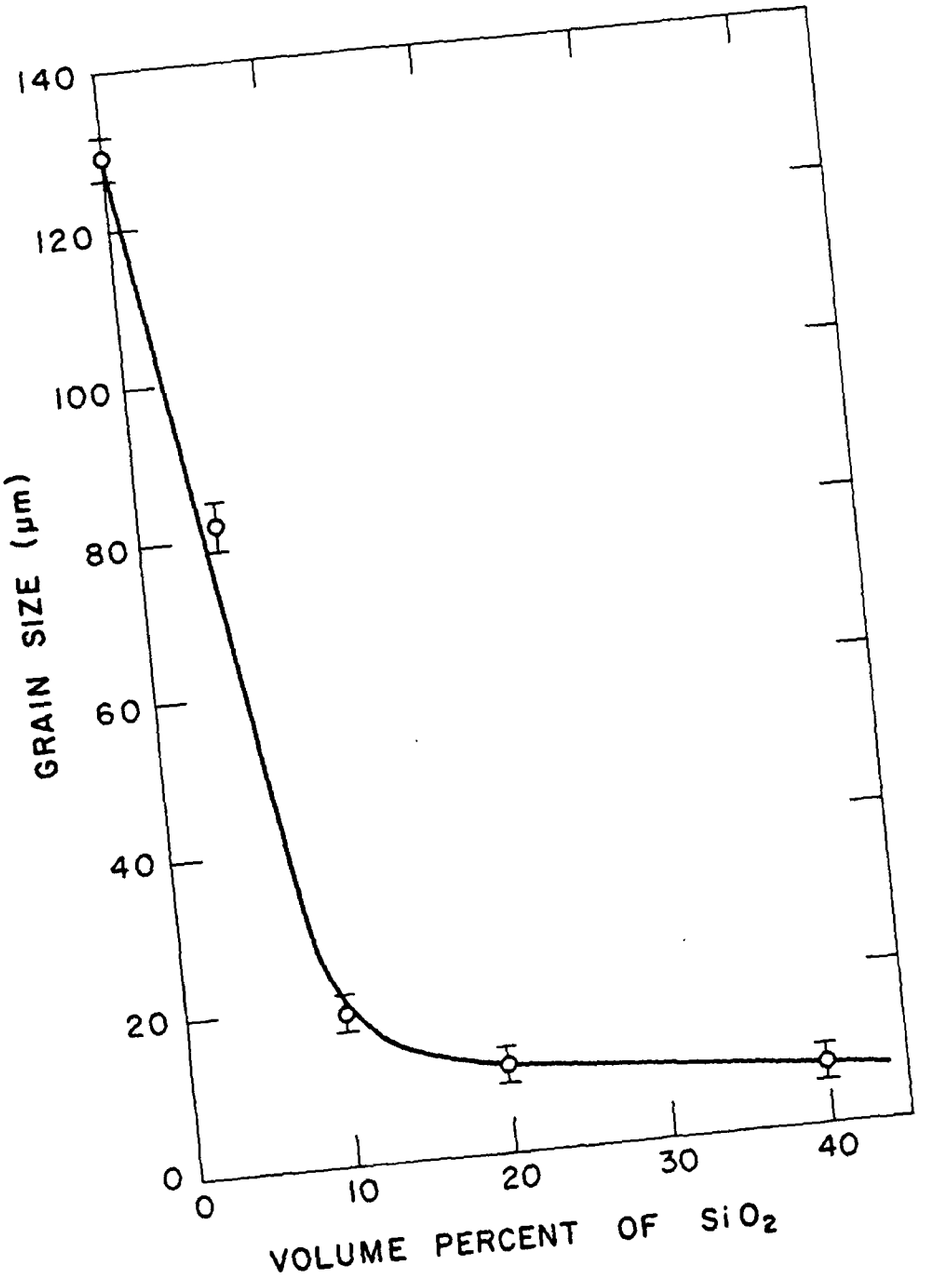

Figure 2. The average grain size plotted as a function of volume percent of SiO_2 in Ni-9Cr alloys.

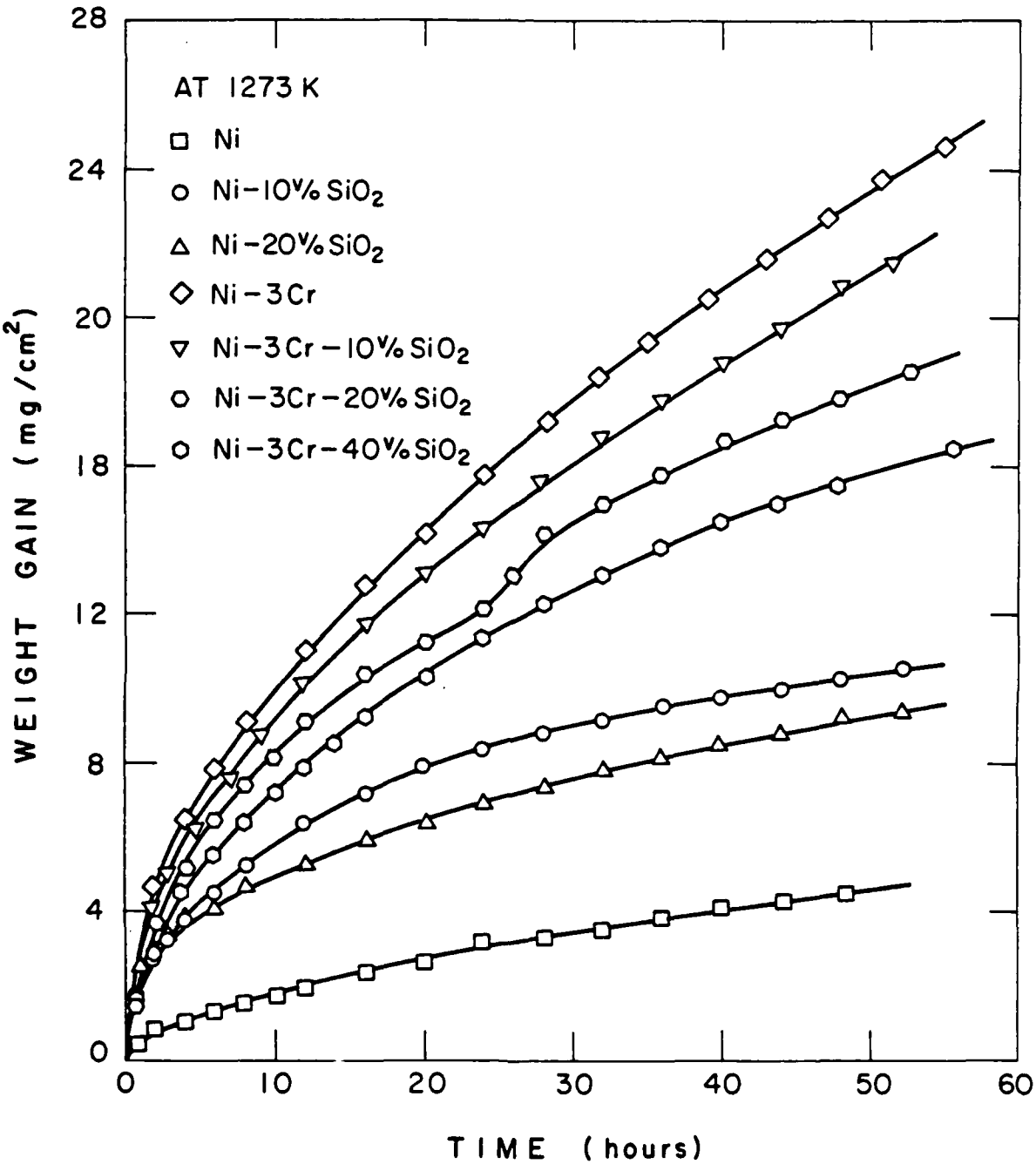

Figure 3. Isothermal oxidation curves for pure Ni and Ni-3Cr alloys with and without SiO_2 as a dispersion at 1273K.

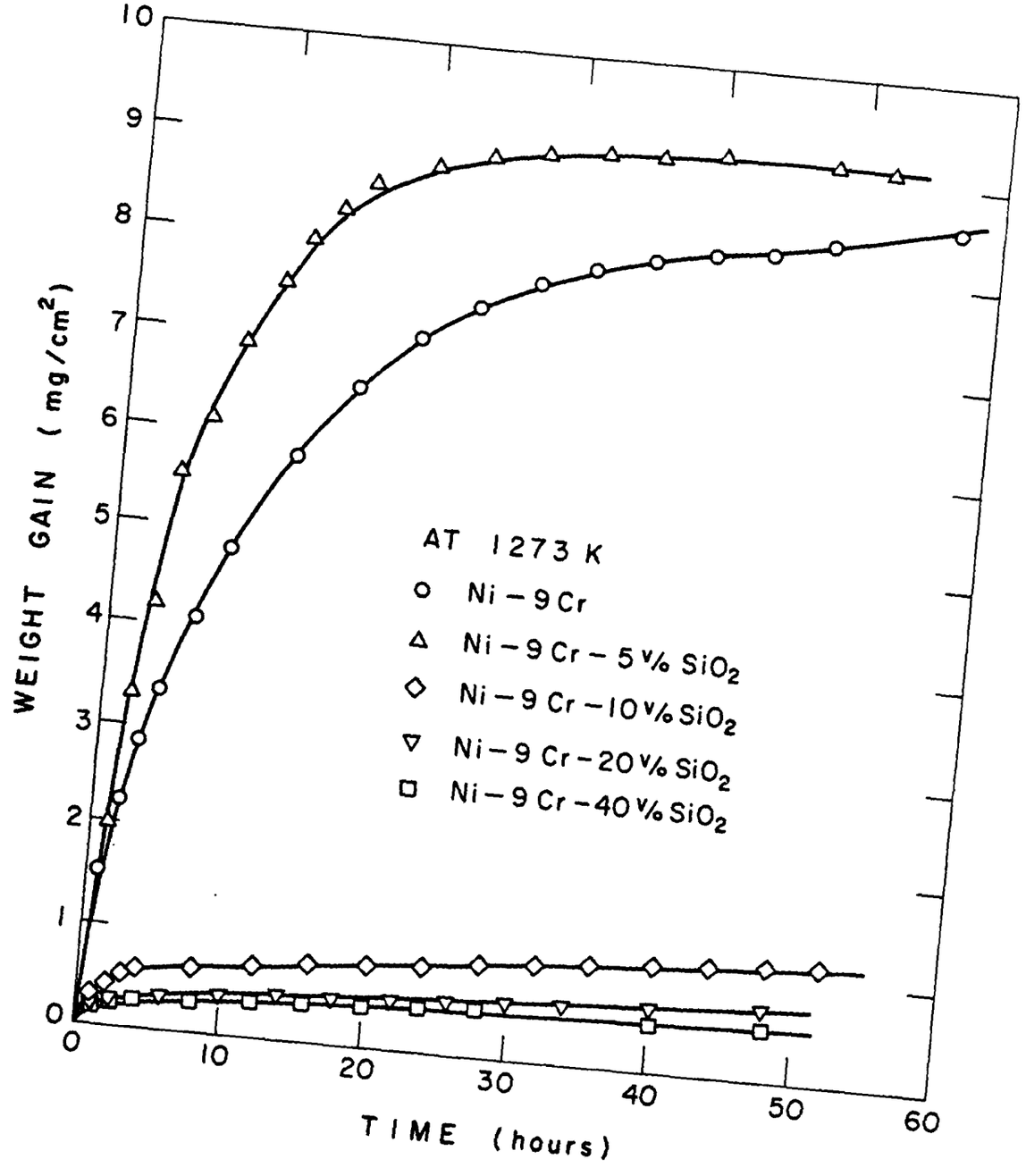

a

Figure 4. Isothermal oxidation curves for Ni-9Cr alloys with and without SiO_2 as a dispersion (a) at 1273K (b) at 1373K in 1 atm O_2.

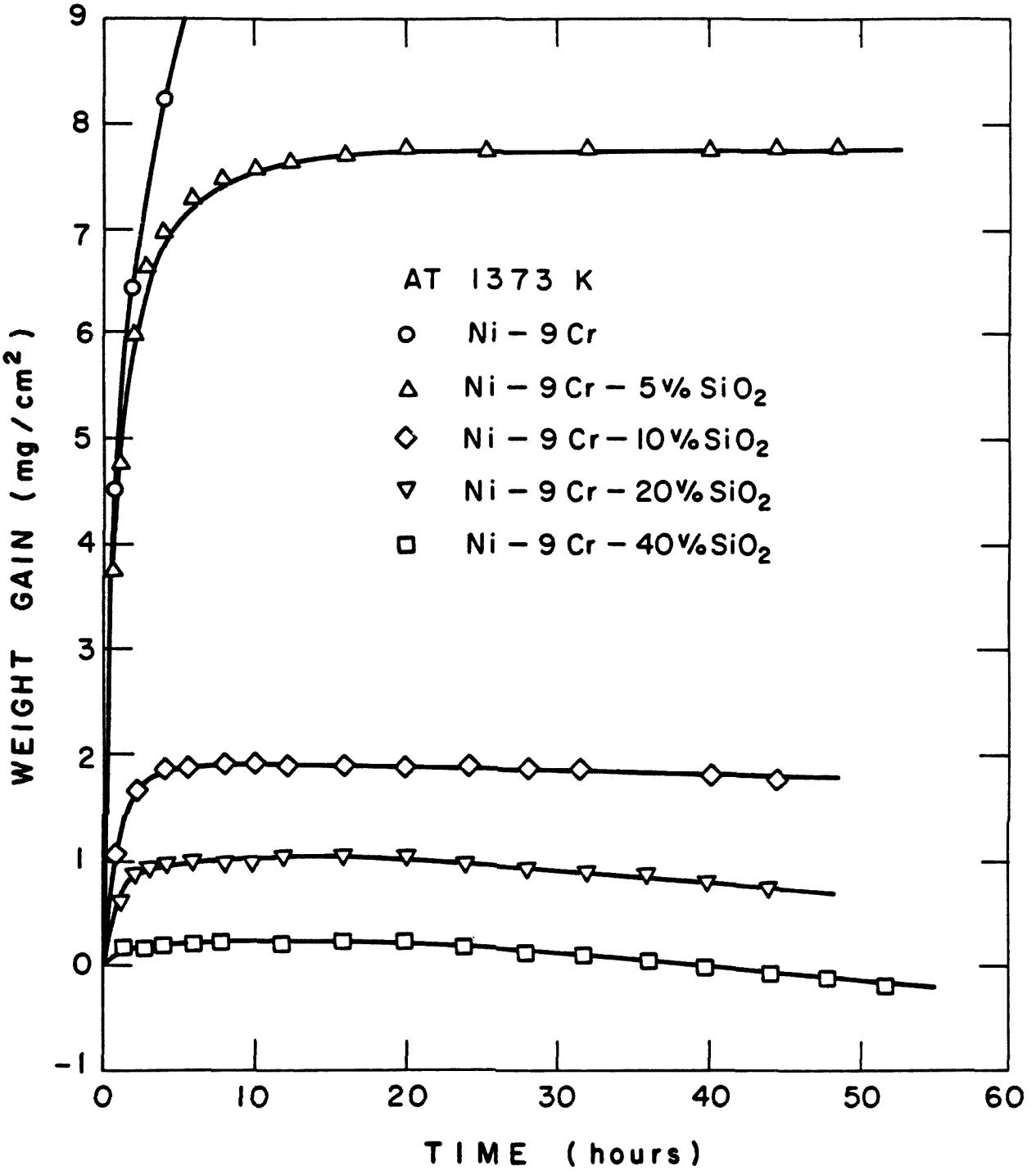

b

Figure 4. Isothermal oxidation curves for Ni-9Cr alloys with and without SiO_2 as a dispersion (a) at 1273K (b) at 1373K in 1 atm O_2.

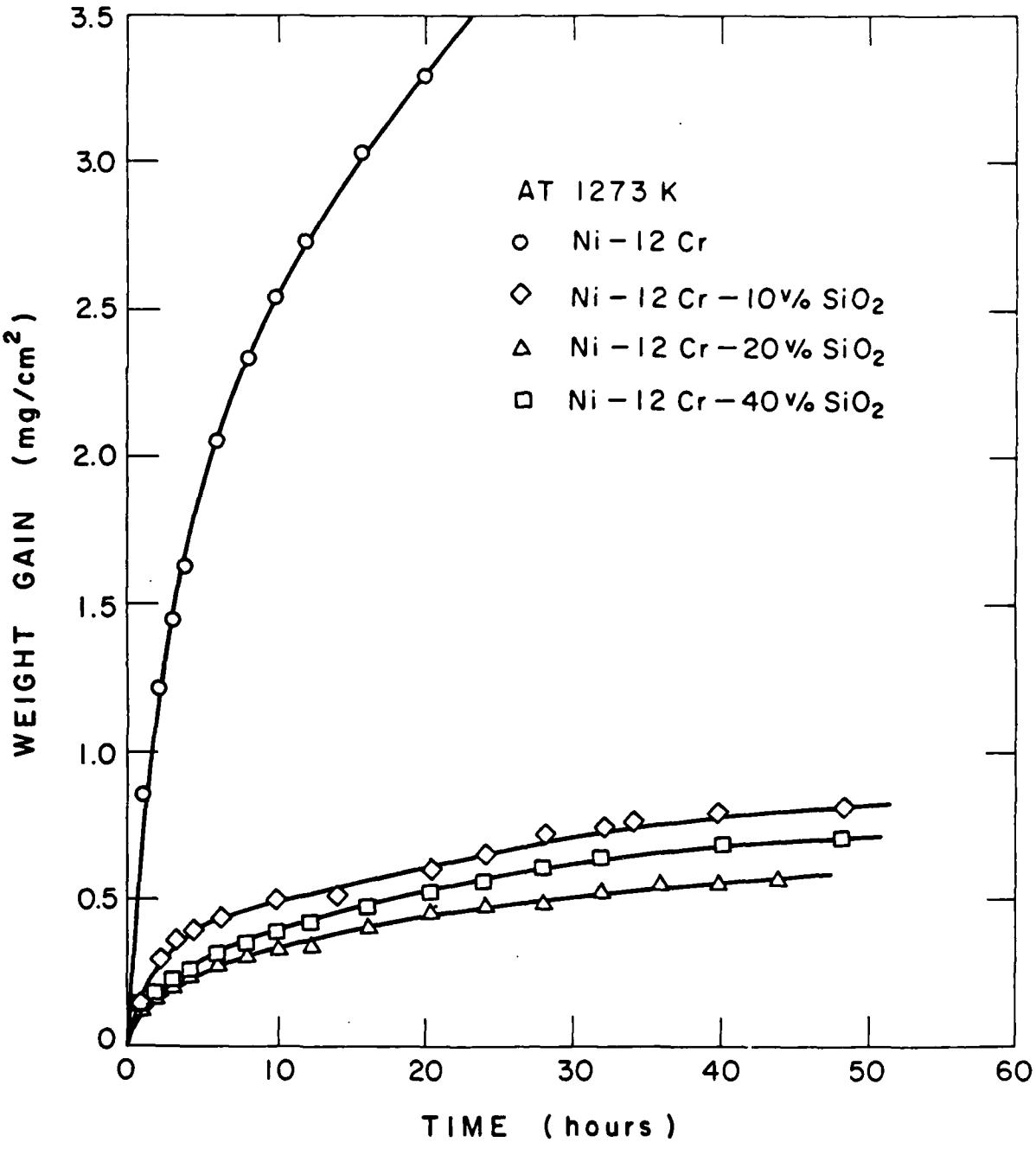

a

Figure 5. Isothermal oxidation curves for Ni-12 Cr alloys with and without SiO_2 as a dispersion (a) at 1273K (b) at 1373K in 1 atm O_2.

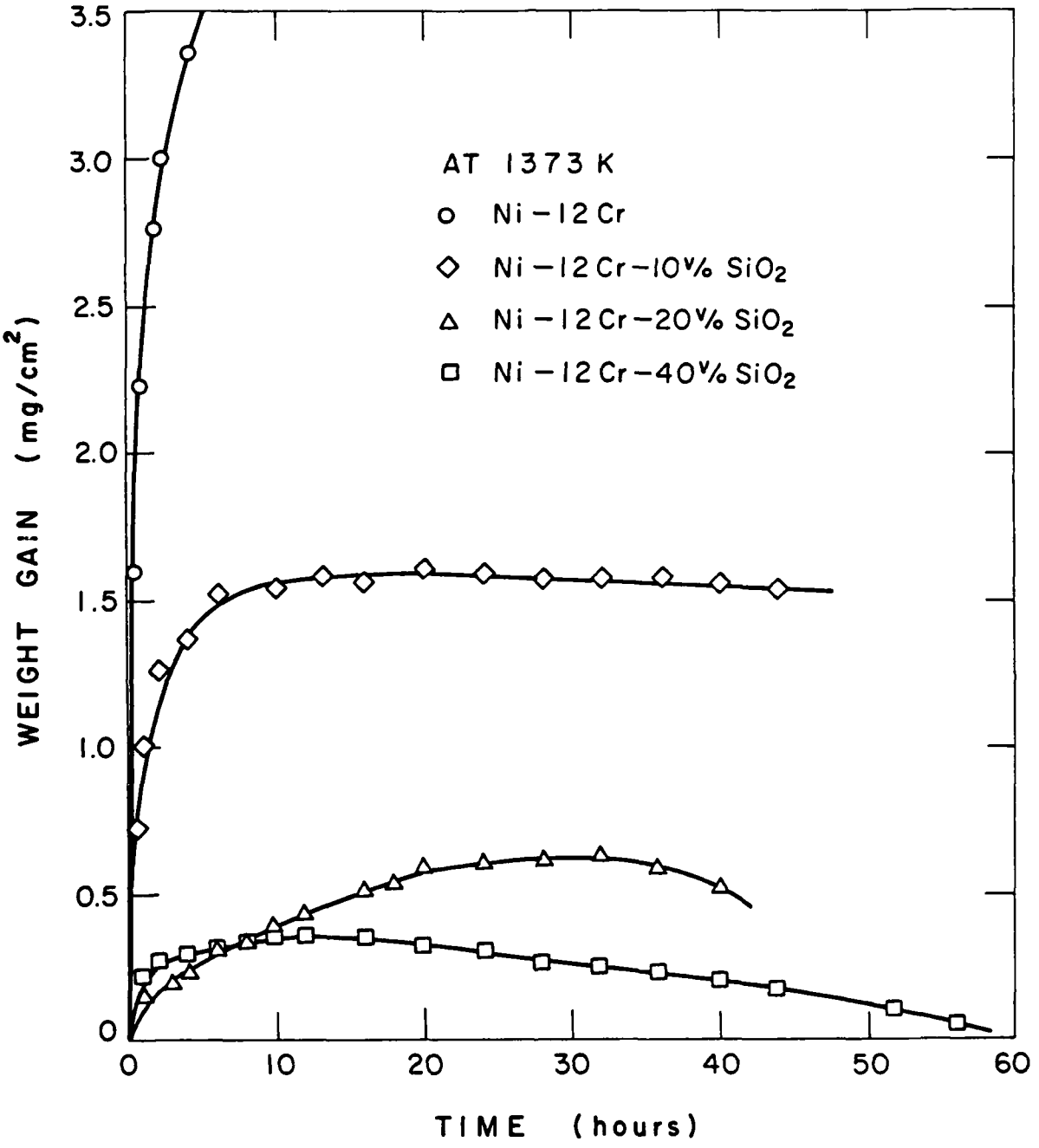

b

Figure 5. Isothermal oxidation curves for Ni-12 Cr alloys with and without SiO_2 as a dispersion (a) at 1273K (b) at 1373K in 1 atm O_2.

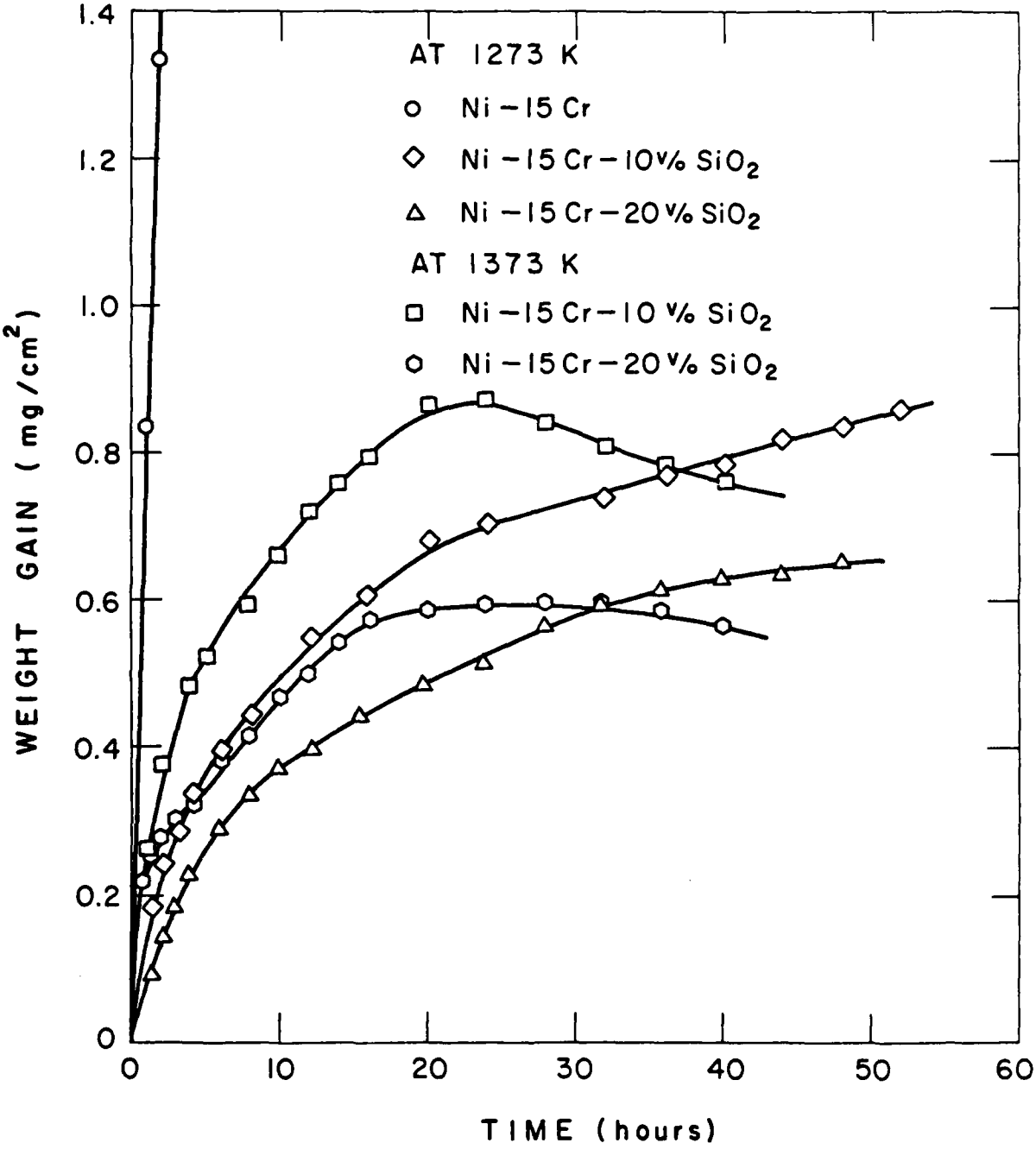

Figure 6. Isothermal oxidation curves for Ni-15Cr alloys with and without SiO_2 as a dispersion at 1273K and 1373 K in 1 atm O_2.

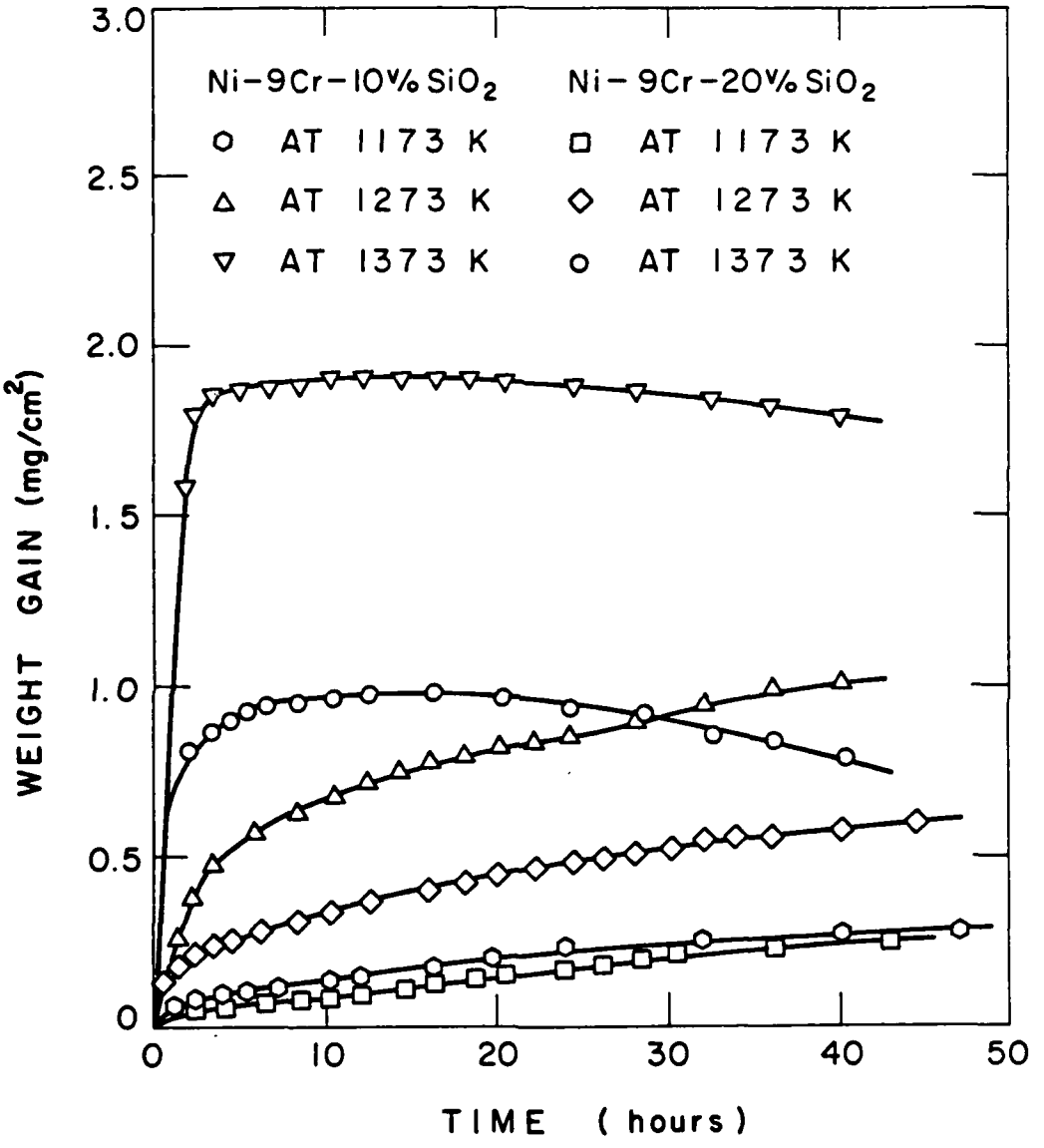

Figure 7. Isothermal oxidation curves for Ni-9Cr-10 vol% SiO_2 and NI-9Cr-20 vol% SiO_2 at various temperatures from 1173K to 1373K.

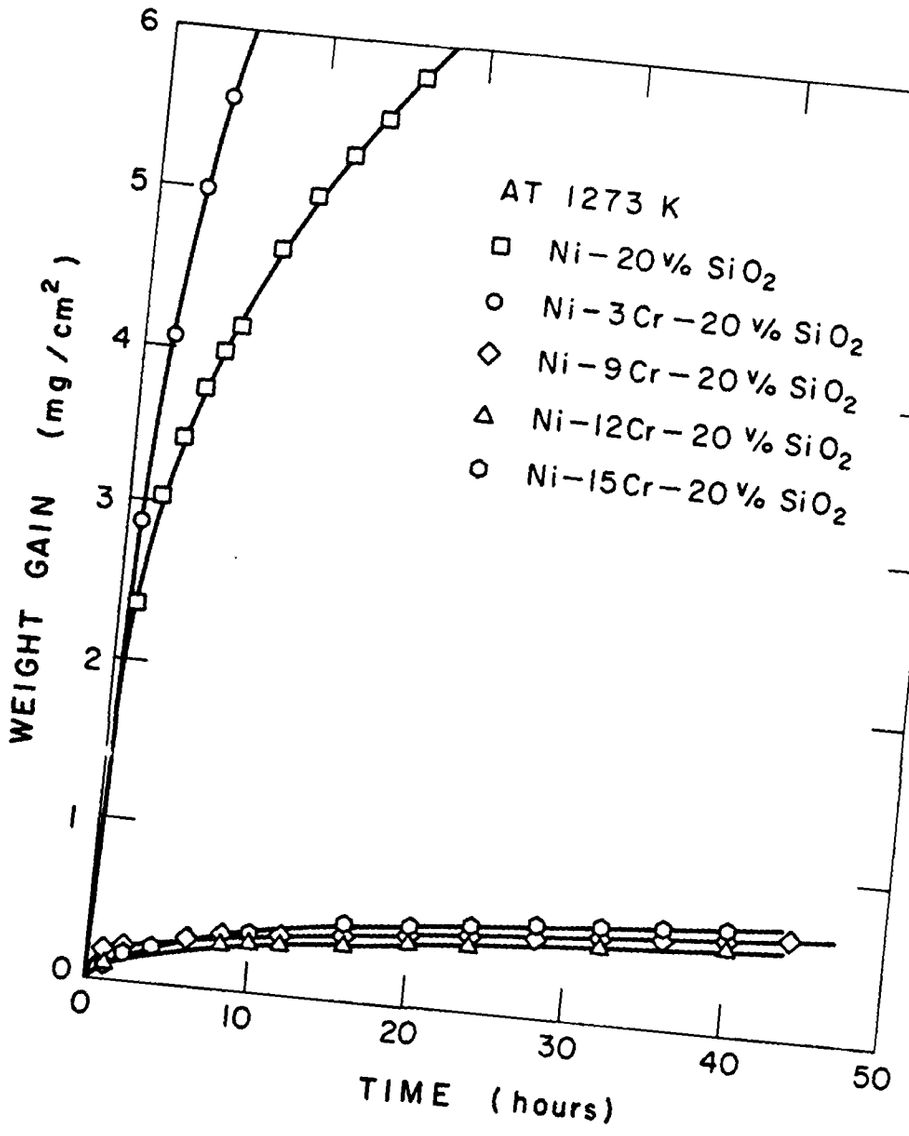

a

Figure 8. Isothermal oxidation curves for Ni-Cr alloys with 20 volume percent of SiO_2 as a function of chromium content (a) at 1273K (b) 1373K.

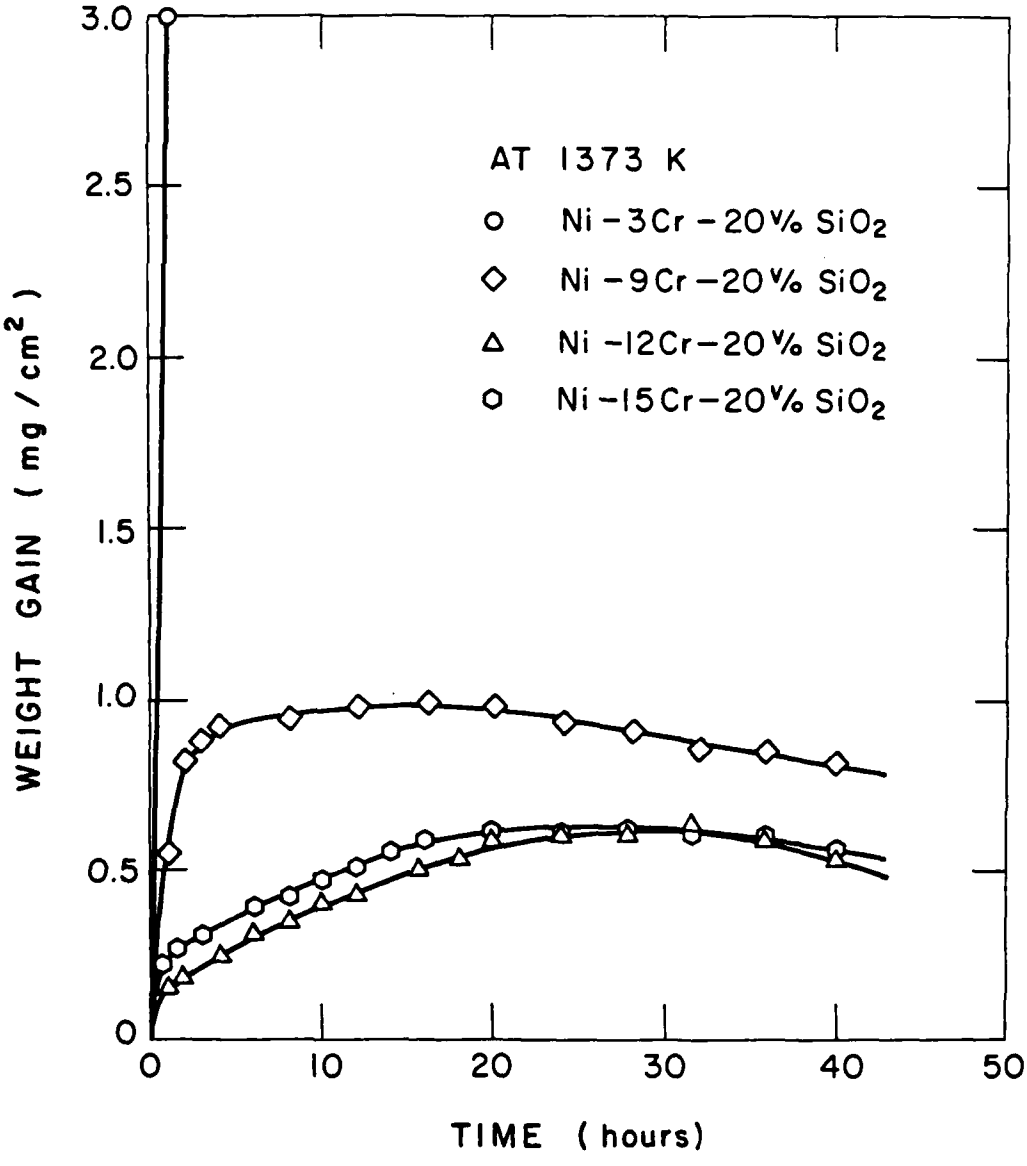

b

Figure 8. Isothermal oxidation curves for Ni-Cr alloys with 20 volume percent of SiO_2 as a function of chromium content (a) at 1273K (b) 1373K.

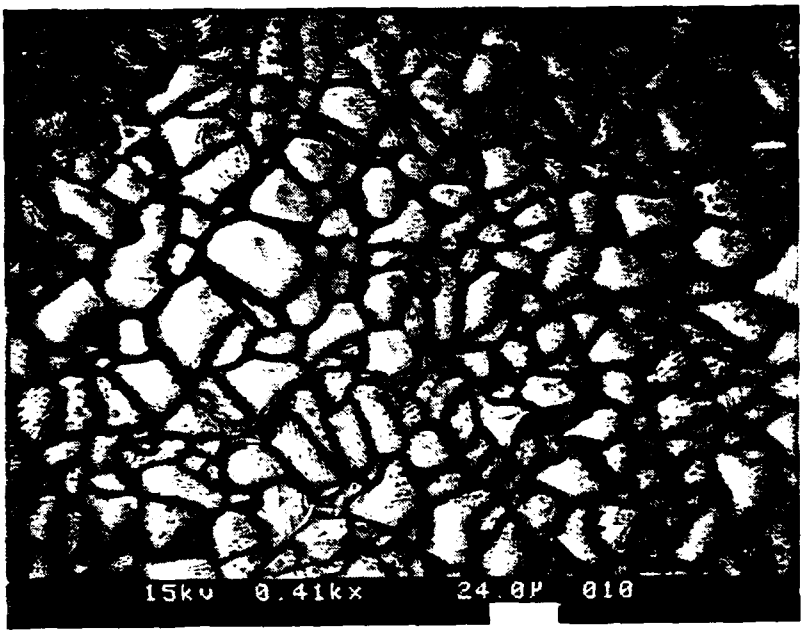

a

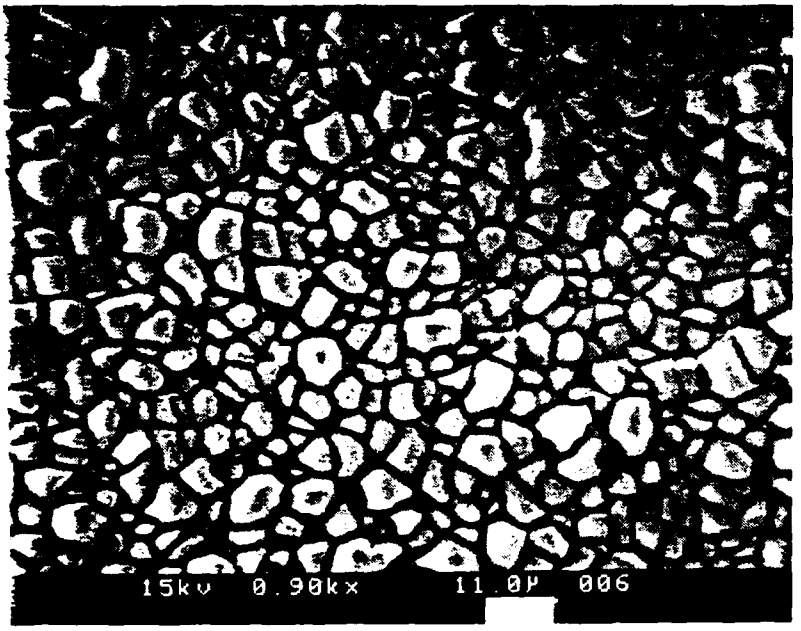

b

Figure 9. Surface topography of (a) pure Ni and (b) pure Ni with 20 volume percent of SiO_2 after 50 hours of oxidation at 1273K.

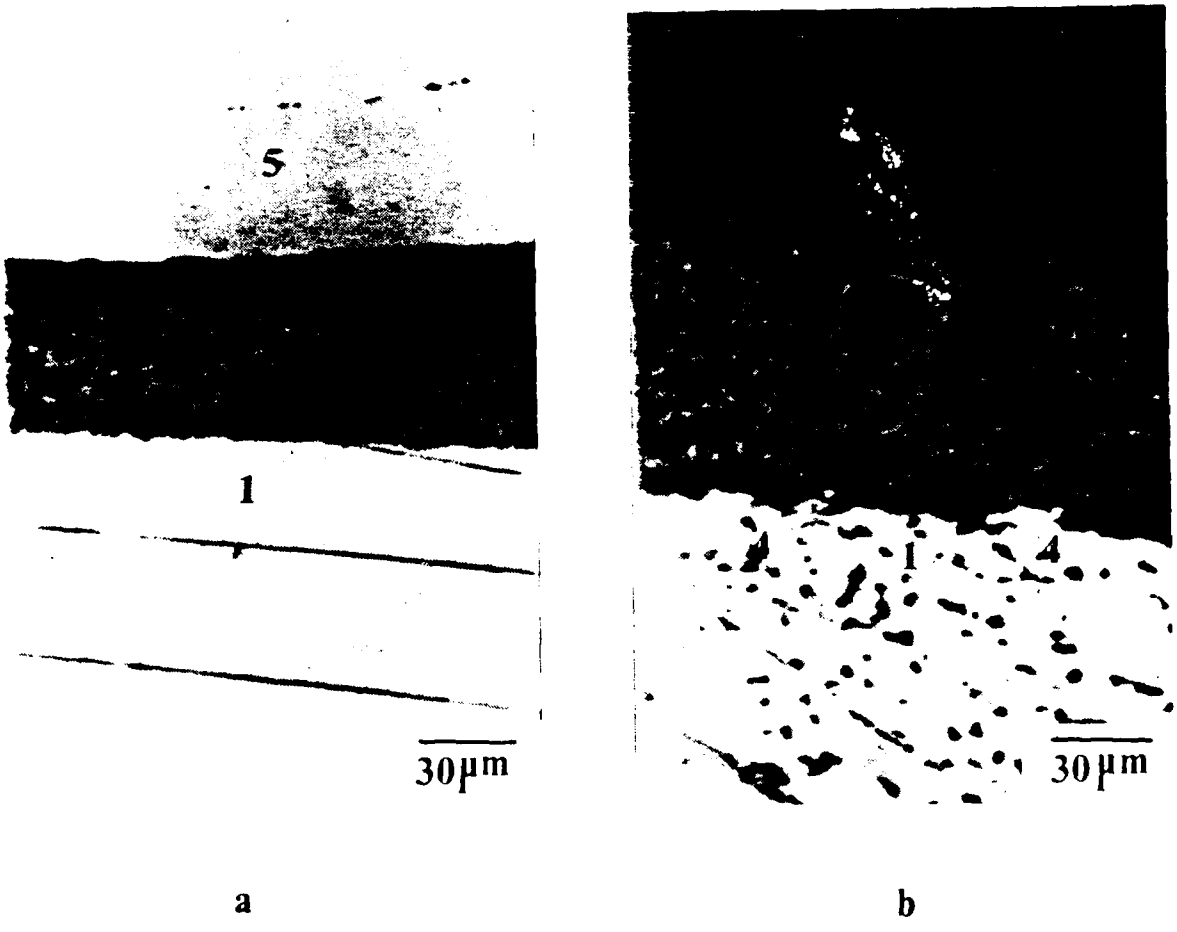

Figure. 10. Cross section of (a) pure Ni, showing a smooth interface and (b) Ni with 20 volume percent of SiO_2, showing that oxides are pegged into the metal matrix, after 50 hours oxidation at 1273K. 1 : matrix 2 : NiO 3 : NiO with SiO_2 4 : SiO_2 5 : mounting material.

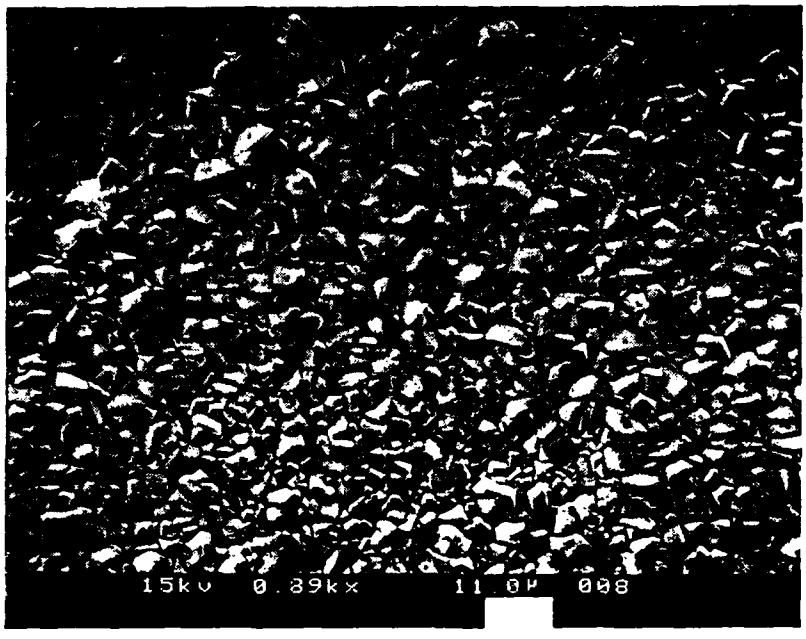

a

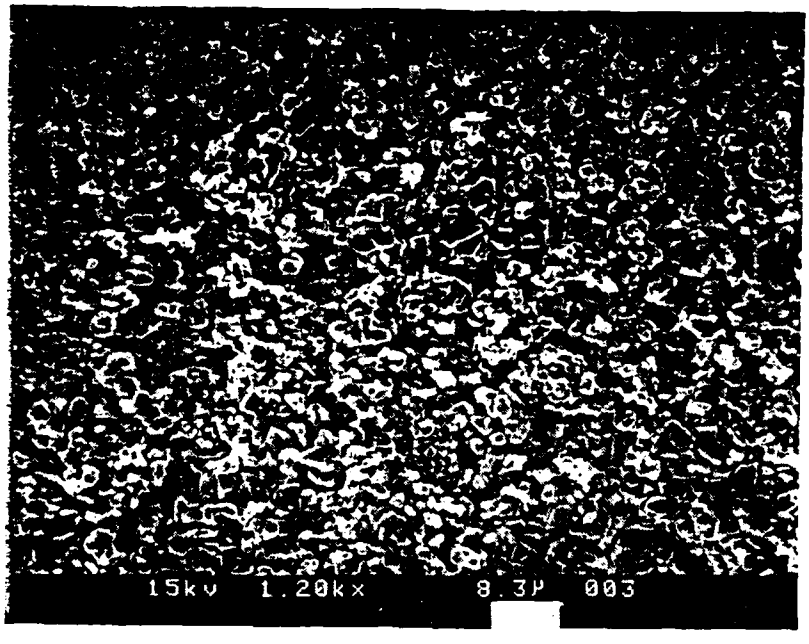

b

Figure 11. (a) Surface topography of binary Ni-9Cr alloy. Surface is entirely covered with NiO.

(b) Surface topography of Ni-9Cr alloy with 20 volume percent of SiO_2. Surface is entirely Cr_2O_3. Oxidation at 1273K for 54 hours.

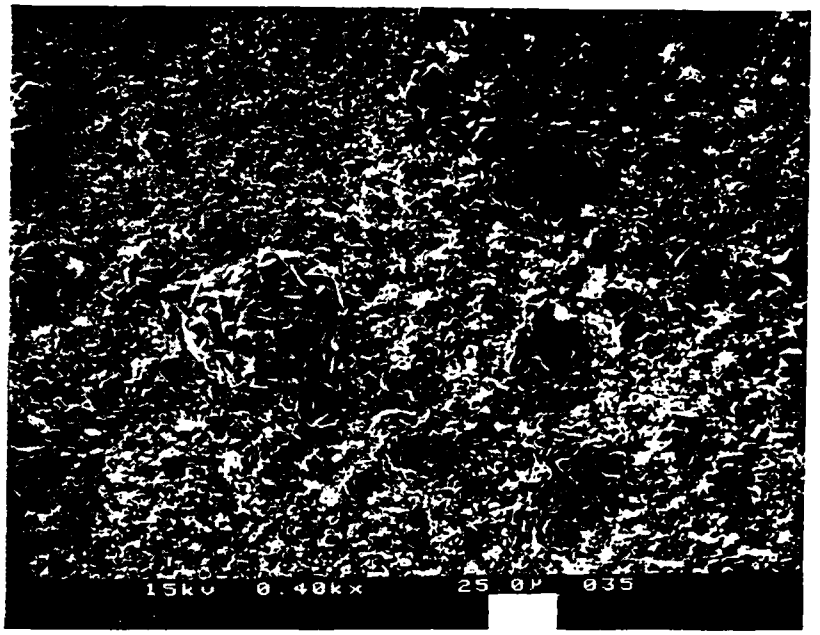

a

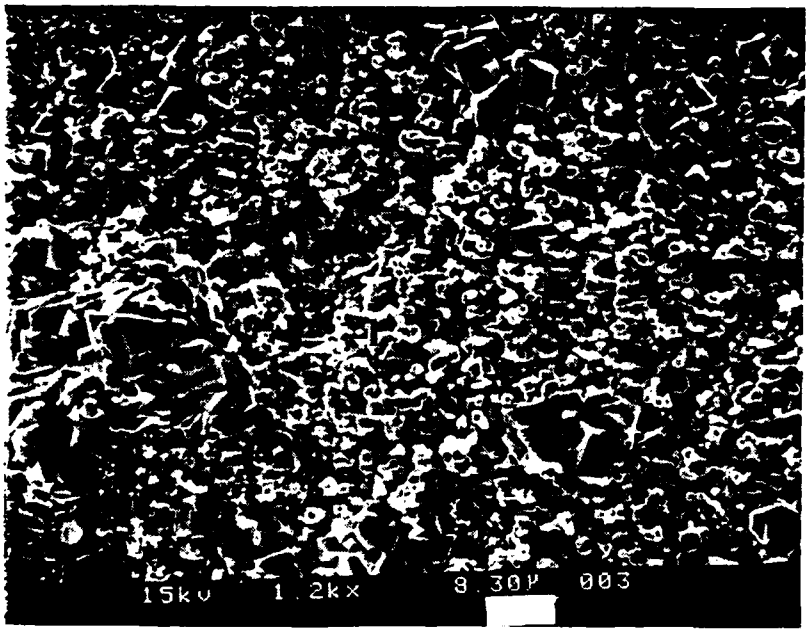

b

Figure 12. Surface topography of Ni-9Cr with 20 volume percent of SiO_2 after oxidation at 1373K for 44 hours. (a) large oxide nodule formed on the oxide surface (b) details of (a) SiO_2 particles appear on oxide surface. 1 : Cr_2O_3 2 : Cr_2O_3/NiO 3 : SiO_2.

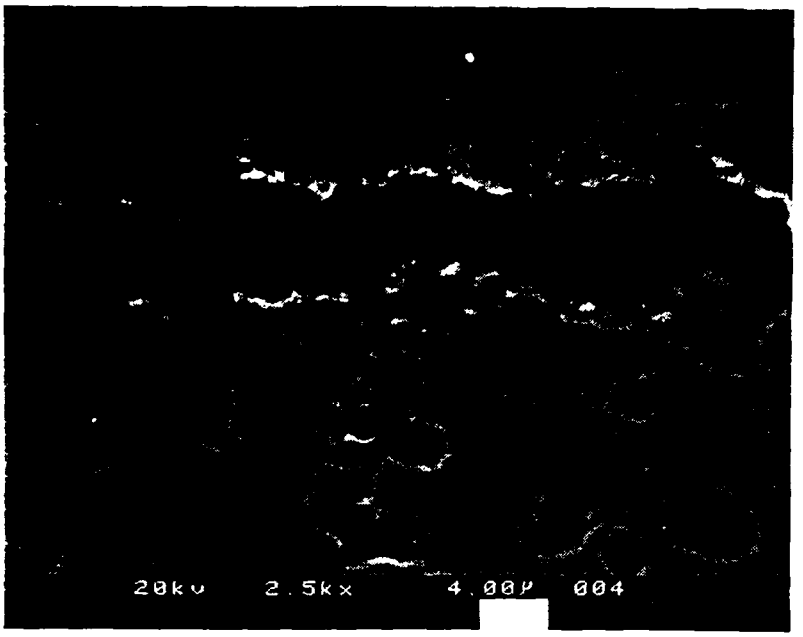

a

b

Figure 13. Cross section of Ni-9Cr alloy (a) with and (b) without 20 volume percent of SiO_2 oxidized at 1273K for 50 hours. 1 : matrix 2 : NiO with $NiCr_2O_4$ 3 : Cr_2O_3 4 : SrO_2 5 : mounting materials 6 : Bi.

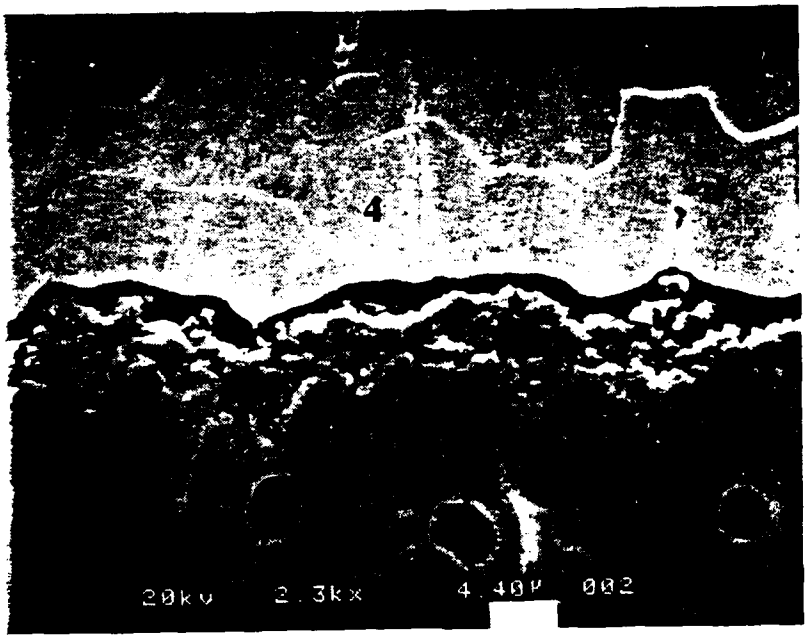

Figure 14. Cross section of Ni-15Cr alloy with 20 volume percent of SiO_2 oxidized at 1273K for 50 hours. 1 : metal matrix 2 : Cr_2O_3 3 : SiO_2 4 : Bi.

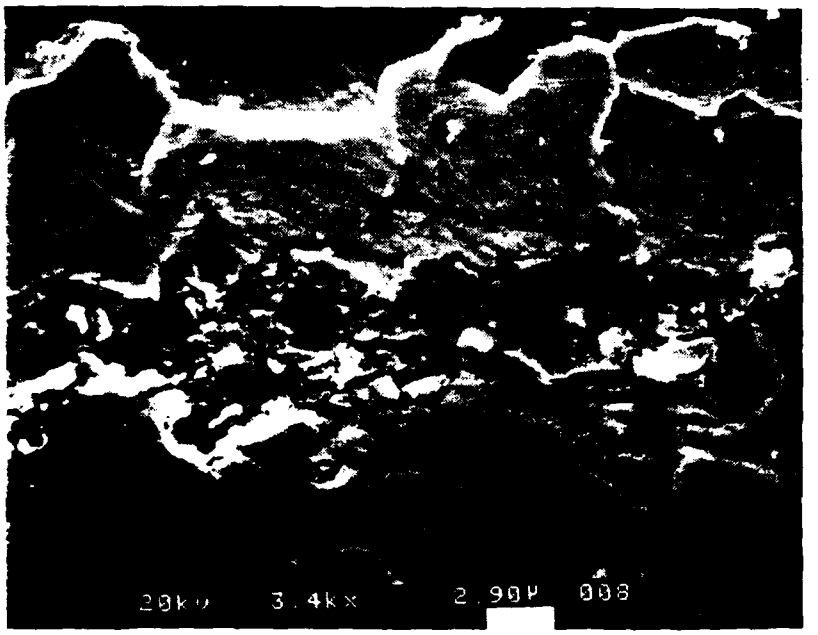

a

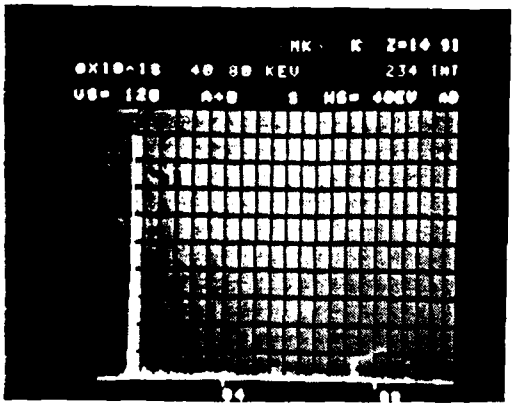

b

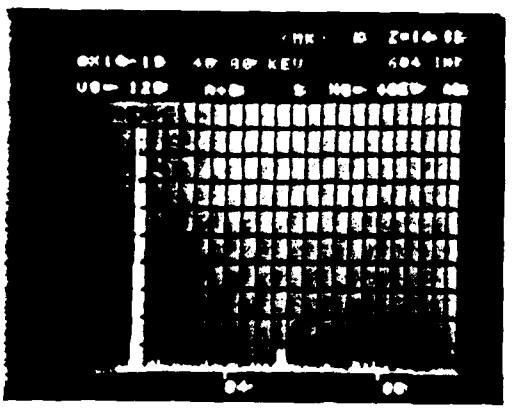

c

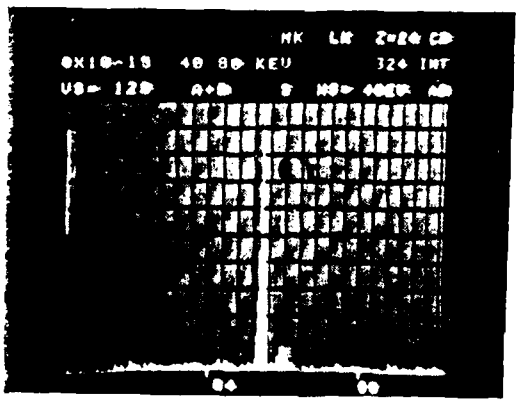

d

Figure 15. (a) Cross section of Ni-12Cr alloy with 40 volume percent of SiO_2 oxidized at 1373K for 60 hours. E.D.S. spectrum for (b) Area A, (c) Area B, (d) Area C. 1 : Metal matrix 2 : Cr_2O_3 3 : SiO_2 4 : Bi.